Geochemistry, Geophysics, Geosystems®

AGU ADVANCING EARTH AND SPACE SCIENCES

REVIEW ARTICLE
10.1029/2022GC010827

Special Section:
A fresh look at the Caribbean plate geosystems

Kinematics and Convergent Tectonics of the Northwestern South American Plate During the Cenozoic

R. González[1,2,3], O. Oncken[1,2], C. Faccenna[1,4], E. Le Breton[2], M. Bezada[5], and A. Mora[6]

[1]Dynamics of the Lithosphere Section, GFZ German Research Centre for Geosciences, Potsdam, Germany, [2]Department of Earth Sciences, Freie Universität Berlin, Berlin, Germany, [3]Ecopetrol, Bogotá, Colombia, [4]Department of Sciences, Roma Tre University, Roma, Italy, [5]Earth & Environmental Sciences, University of Minnesota, Minneapolis, MN, USA, [6]Ecopetrol, Rio de Janeiro, Brazil

Abstract The interaction of the northern Nazca and southwestern Caribbean oceanic plates with northwestern South America (NWSA) and the collision of the Panama-Choco arc (PCA) have significant implications on the evolution of the northern Andes. Based on a quantitative kinematic reconstruction of the Caribbean and Farallon/Farallon-derived plates, we reconstructed the subducting geometries beneath NWSA and the PCA accretion to the continent. The persistent northeastward migration of the Caribbean plate relative to NWSA in Cenozoic time caused the continuous northward advance of the Farallon-Caribbean plate boundary, which in turn resulted in its progressive concave trench bending against NWSA. The increasing complexity during the Paleogene included the onset of Caribbean shallow subduction, the PCA approaching the continent, and the forced shallow Farallon subduction that ended in the fragmentation of the Farallon Plate into the Nazca and Cocos plates and the Coiba and Malpelo microplates by the late Oligocene. The convergence tectonics after late Oligocene comprised the accretional process of the PCA to NWSA, which evolved from subduction erosion of the forearc to collisional tectonics by the middle Miocene, as well as changes of convergence angle and slab dip of the Farallon-derived plates, and the attachment of the Coiba and Malpelo microplates to the Nazca plate around 9 Ma, resulting in a change of convergence directions. During the Pliocene, the Nazca slab broke at 5.5°N, shaping the modern configuration. Overall, the proposed reconstruction is supported by geophysical data and is well correlated with the magmatic and deformation history of the northern Andes.

Plain Language Summary The tectonic reconstruction in convergent triple junctions is a particularly challenging task as the relative motion between plates could define highly changing boundaries. Indeed, the resulting interaction between these convergent plates may induce important changes in the disposition of the trenches, and in turn in the three-dimensional geometry of the subducting plates. Therefore, these highly dynamic conditions throughout geological time may be accommodated by different phases of plate fragmentation and reorganization. These factors could explain the complex spatial-temporal distribution of subduction-related magmatism and the different episodes of deformation in the upper plates. This reasoning is validated in the northwestern corner of South America (SA), where the continent has been converging against the Caribbean and Farallon-derived oceanic plates since Cretaceous time. Additionally, we study the effects of the collision and accretion of the Panama-Choco arc with SA. To accomplish that, we review the kinematic history of the Farallon/Nazca and Caribbean oceanic plates relative to stable Guiana Craton (SA) and integrate these results with the magmatic and deformation evolution of the northern Andes, which allow us to propose a model of the geometrical evolution of the subducting slabs. The obtained model is additionally constrained by seismological data and published velocity anomalies.

Key Points:

- The tectonics of convergent triple junctions is complicated by the relative plate motion and interaction of the involved plates
- We propose a model for the kinematic and geometric evolution of the Farallon/Nazca and Caribbean plates throughout the Cenozoic
- The interaction between the Caribbean, Nazca and South American plates is closely related to the deformation history in the Northern Andes

Supporting Information:

Supporting Information may be found in the online version of this article.

Correspondence to:

R. González,
rgonzal@gfz-potsdam.de

Citation:

González, R., Oncken, O., Faccenna, C., Le Breton, E., Bezada, M., & Mora, A. (2023). Kinematics and convergent tectonics of the Northwestern South American plate during the Cenozoic. *Geochemistry, Geophysics, Geosystems*, *24*, e2022GC010827. https://doi.org/10.1029/2022GC010827

Received 12 DEC 2022
Accepted 26 MAY 2023

Author Contributions:

Conceptualization: R. González, A. Mora
Formal analysis: R. González
Methodology: R. González, O. Oncken, C. Faccenna, E. Le Breton

1. Introduction

From a regional point of view, it is recognized that topographic and structural style differences in the Andean range throughout South America (SA) are due to lateral variations of convergence parameters between the Farallon/Nazca and the continent (Figure 1) (e.g., Cediel et al., 2003; Gansser, 1973; Oncken et al., 2006; Ramos, 2010; Trumbull et al., 2006). The most important element that characterizes the tectonic evolution of the northern Andes is that the Nazca subduction is complicated by its interaction with the Caribbean plate since Cretaceous time (Figure 1) (e.g., Burke, 1988; Mann, 1999; J. L. Pindell & Barrett, 1990), conforming a triple junction with SA. Furthermore, the tectonic setting in this region is conditioned by the collision of the Panama-Choco

Resources: O. Oncken, C. Faccenna, M. Bezada
Software: E. Le Breton, M. Bezada
Supervision: O. Oncken, C. Faccenna
Validation: O. Oncken, C. Faccenna, E. Le Breton, M. Bezada, A. Mora
Writing – original draft: R. González
Writing – review & editing: R. González, O. Oncken, C. Faccenna, A. Mora

arc (PCA) since the late Oligocene (Farris et al., 2011; Montes et al., 2012). Within this context, the subduction geodynamics of the Nazca and Caribbean plates should not be simplified as the independent subduction of two oceanic slabs beneath the continent, but as a triple junction that should be addressed in a three-dimensional framework. Indeed, several authors (e.g., Faccenna et al., 2018; Toda et al., 2008) have demonstrated that the interaction between subducting slabs in similar convergent triple junctions has major tectonic implications on the tectonic evolution of the upper plate. Therefore, to decipher the tectonic evolution of northwestern SA, it is necessary to understand the development of the involved plates at this triple junction.

A fundamental question to understand the tectonics of Northwestern South America (NWSA) is the present-day configuration of the subducting plates. Several studies on the distribution of seismic events in the northern Andes (e.g., Chiarabba et al., 2015; Sun et al., 2022; Taboada et al., 2000) have led to several competing models on the geometric configuration of the transition between the Nazca and Caribbean plates at depth (Figure 2) (e.g., Kellogg et al., 2019; Pennington, 1981; Sun et al., 2022; Syracuse et al., 2016; Vargas & Mann, 2013). While some models support a shear zone between the Caribbean and Nazca slabs at 5.5°N (Figures 3 and 4) (Pennington, 1981), implying the abrupt termination of both plates at this position, other models favor an overlapping region between these slabs (e.g., Cortés & Angelier, 2005; Sun et al., 2022; Taboada et al., 2000; Vargas, 2019).

As a consequence of relative plate motions, it is expected that convergent triple junctions do not behave as static elements in time (Faccenna et al., 2018). Though this factor is not understood at the Caribbean, SA and Pacific plates (CSP) triple junction (Figure 3a), it is important to reckon the possible scenarios of a triple junction that moved in time or a triple junction that remained static, which have huge implications for the northern Andes

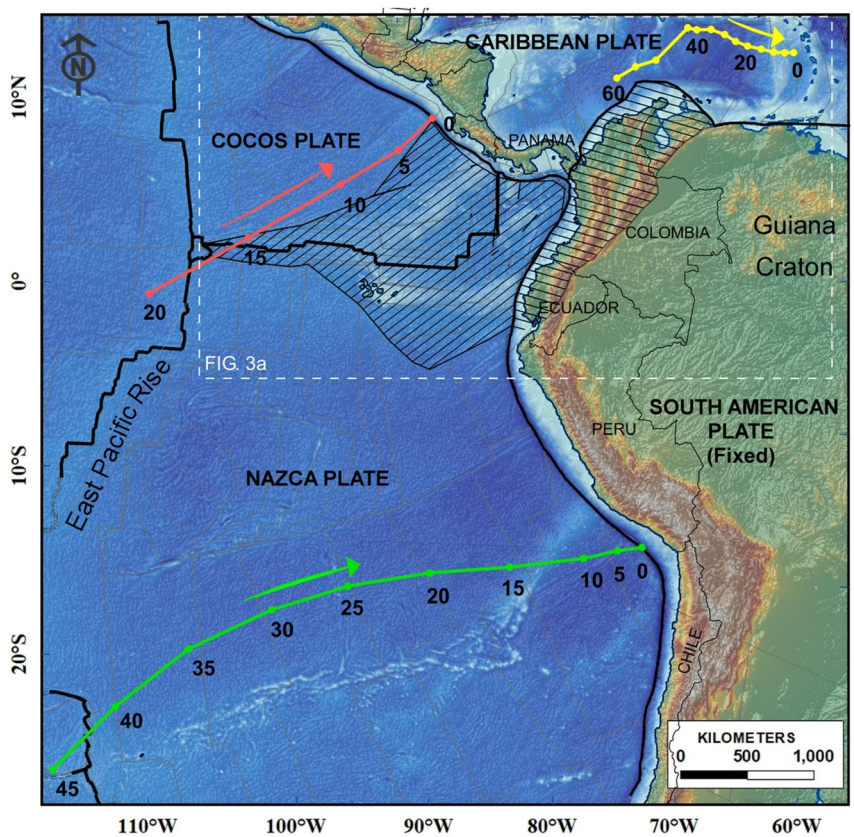

Figure 1. Regional tectonic map of the South and Central American subduction zones showing the plate boundaries. Color lines show plate displacement vectors during the Cenozoic, according to existing paleotectonic models for the Farallon/Nazca (green; Müller et al., 2019), Cocos (red; Müller et al., 2019), and Caribbean (yellow; Boschman et al., 2014) plates. Numbers refer to the reconstructed positions throughout time (Ma) relative to stable South America (SA). The dashed area within the Nazca-Cocos plates shows the Miocene to Recent crust erupted from the Nazca-Cocos spreading center. The dashed area within the South American plate highlights the Northern Andes area. Digital elevation model from Amante and Eakins (2009).

10.1029/2022GC010827

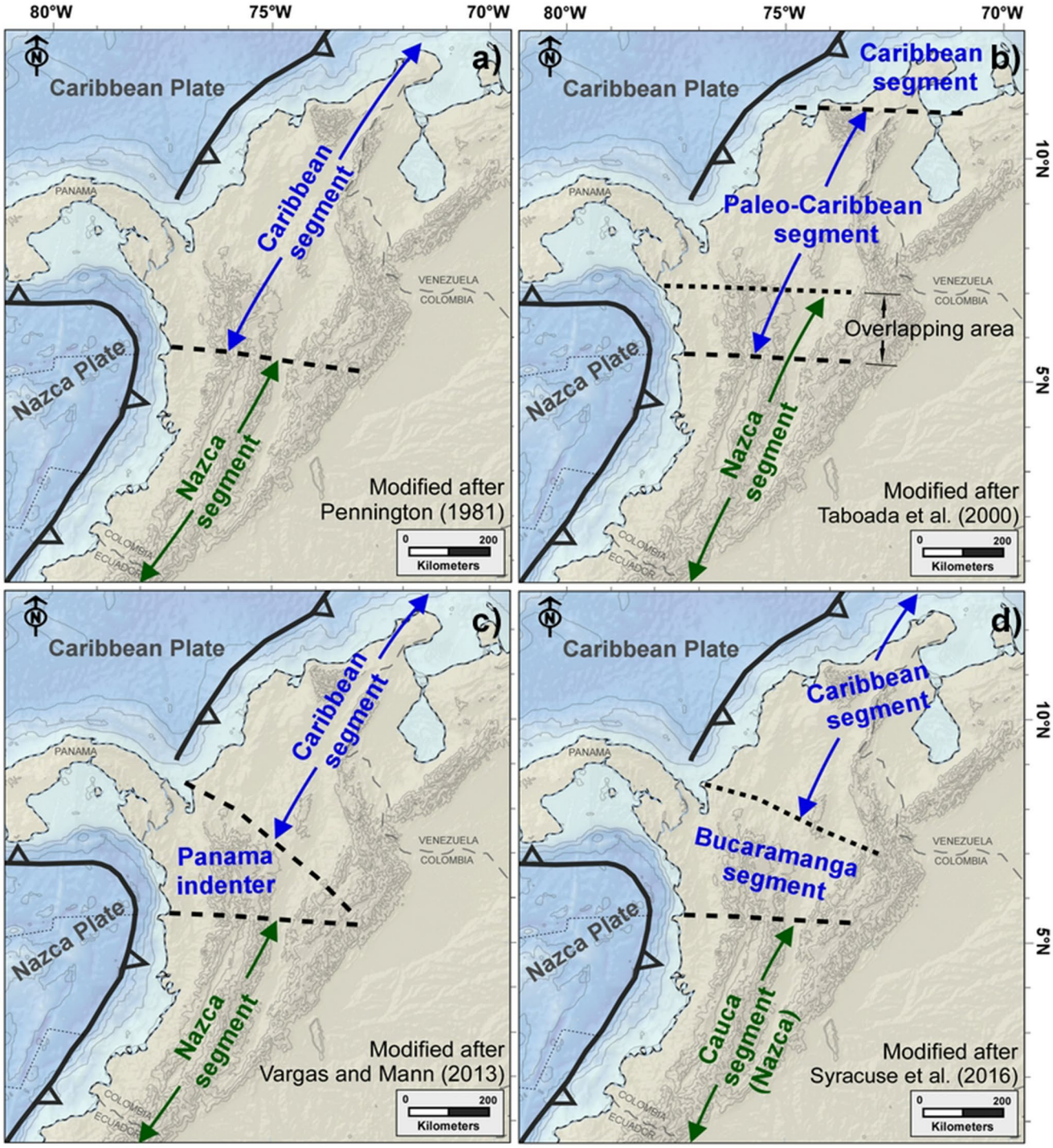

Figure 2. Some previous interpretations showing the existing ambiguity in the definition of the slab boundaries beneath South America (SA). Generalized models proposed by (a) Pennington (1981), (b) Taboada et al. (2000), (c) Vargas and Mann (2013) and (d) Syracuse et al. (2016). While several authors consider the northern edge of the Nazca plate to be at about 5.5°N (e.g., Pennington, 1981), others prefer more northerly positions (Cortés & Angelier, 2005; Sun et al., 2022; Taboada et al., 2000). The southern edge of the Caribbean plate is also ambiguous, as some interpretations delineate this boundary at 5.5°N. In contrast, other authors consider the Caribbean slab to be as south as 4°N (Kellogg et al., 2019; Sun et al., 2022), in agreement with the southern occurrence of Miocene accreted rocks of the Panama-Choco arc. The Panama indenter and the Bucaramanga segment (c, d) are derived from the Caribbean plate after its convergence against SA (Syracuse et al., 2016; Vargas & Mann, 2013).

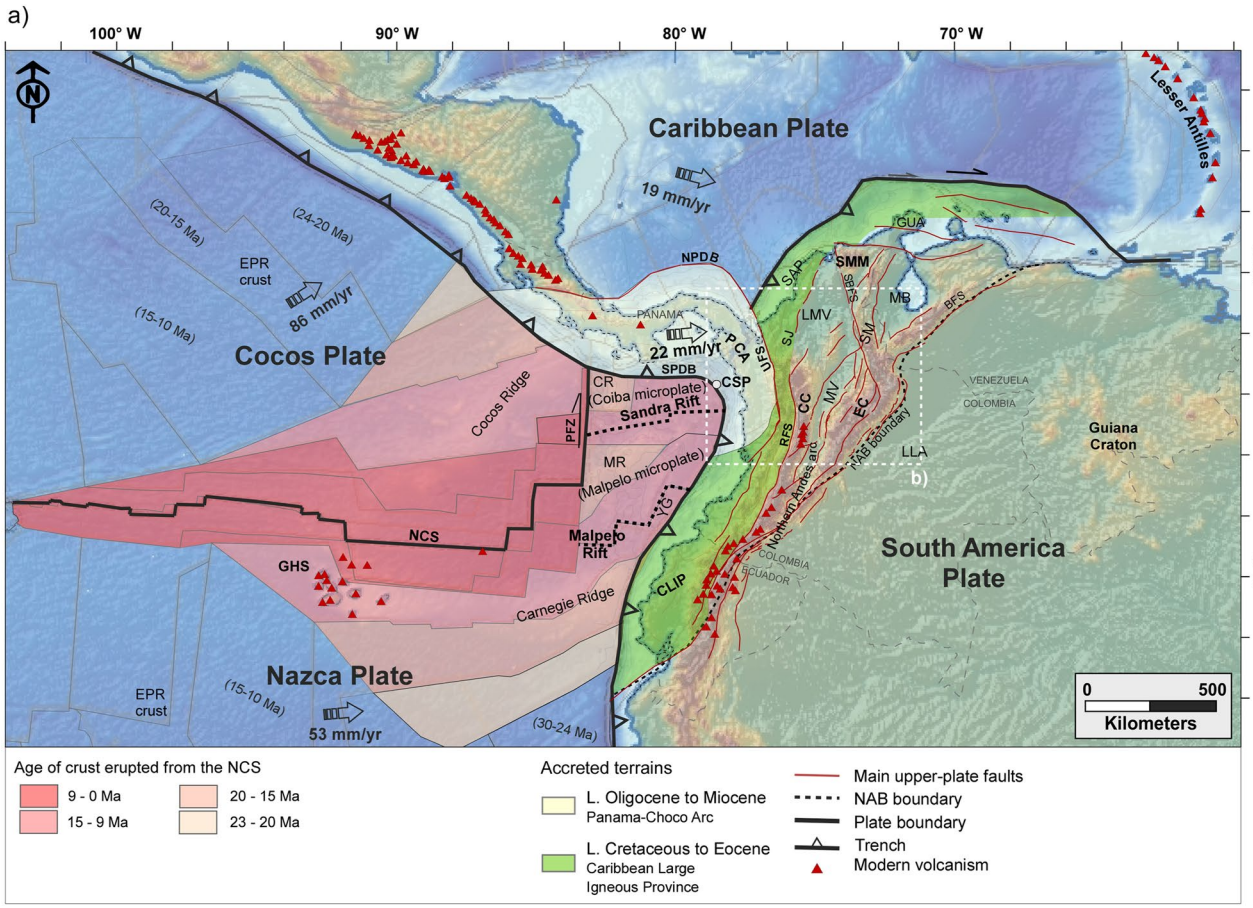

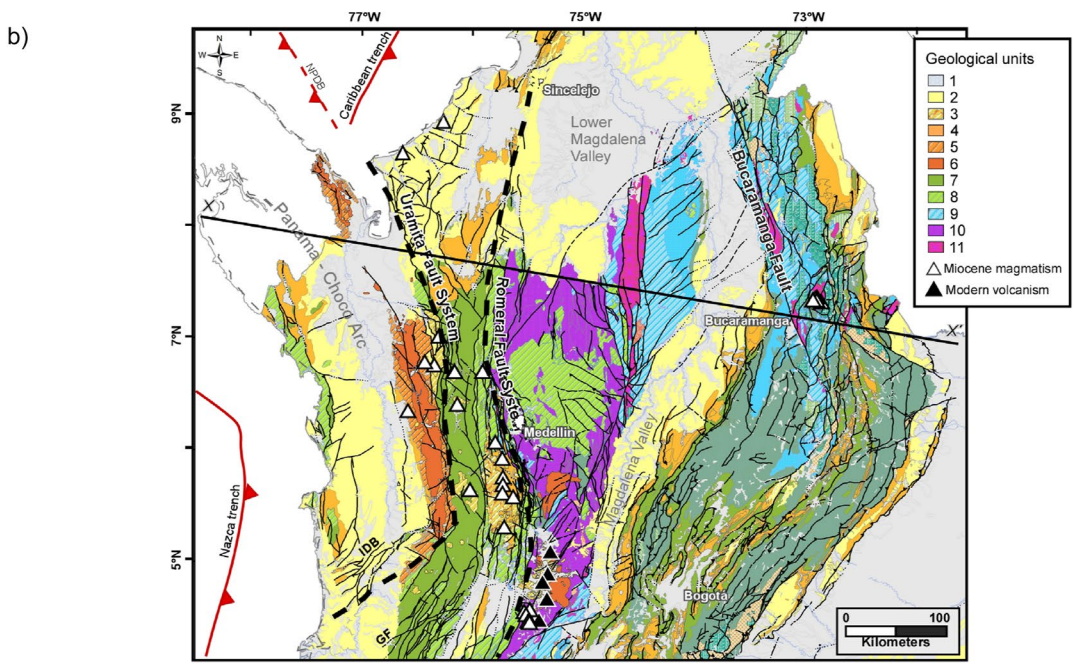

Figure 3.

evolution. In this regard, it is necessary to consider the origin of the Caribbean plate, which has been interpreted as an autochthonous oceanic plate (Meschede & Frisch, 1998), and as an allochthonous plate that migrated from the Pacific region (e.g., Burke, 1988). We prefer the interpretation of the allochthonous oceanic plate as it is in accordance with different paleomagnetic and geological evidence (Escalona & Mann, 2011; Farris et al., 2011; Montes et al., 2012; J. L. Pindell & Kennan, 2009) and additionally, it is well constrained by the plate motion network suggested by recent global and regional plate reconstruction models (e.g., Boschman et al., 2014; Müller et al., 2019; Seton et al., 2012). Based on the above, in this paper, we assume that the CSP triple junction (Figure 3) was not static but changed its position throughout the Cenozoic.

Furthermore, the relative motion of the Farallon/Farallon-derived plates also plays an important role in the definition of the southwestern boundary of the Caribbean plate and the position of the CSP triple junction (CSP) (Figure 3a). However, the Nazca plate kinematics is well constrained between 10°S and 21°S (Figure 1) (e.g., Pardo-Casas & Molnar, 1987; Somoza & Ghidella, 2012), but the plate motion history is poorly understood in the area corresponding to the Coiba and Malpelo microplates (Figure 3a). In this region, the kinematics was complicated by an intricate crustal spreading history after the breakup of the Farallon plate (e.g., Geldmacher et al., 2013; Handschumacher, 1976; Lonsdale, 2005; MacMillan et al., 2004; Sallarès et al., 2003). Undoubtedly, a different motion history of the present-day northern Nazca plate (former Coiba and Malpelo microplates) (Figure 3a) as compared with southern latitudes has huge regional implications that demand a thorough debate.

In this contribution, we review the kinematic reconstruction of the subducting Farallon/Nazca and Caribbean plates relative to SA throughout the Cenozoic. In order to discuss the intricate tectonic history of this region, we present the kinematic analysis for the Caribbean and the other Farallon-derived plates in chronological order, and then we discuss the interacting influence between them and their role on the spatial and temporal patterns of magmatism and first order deformation episodes in the northern Andes. Finally, the present-day slab geometries resulting from our kinematic reconstruction are validated with a recent tomographic model that allows us to propose an alternative interpretation of the current tectonic configuration beneath NWSA.

2. Tectonic Setting

2.1. The Southwestern Caribbean Plate and the Panama-Choco Arc (PCA)

The Caribbean plate is a thick and buoyant oceanic plateau (e.g., J. Pindell et al., 2005), which according to the hypotheses of allochthonous origin (Burke, 1988), was formed during the Late Cretaceous in the eastern Pacific region, and subsequently migrated eastwards between the North and South American plates. During its migration, the oblique convergence triggered the diachronous accretion of the oceanic terrains known as the Caribbean Large Igneous Province (CLIP; Figure 3) (Cediel et al., 2003; Etayo-Serna, 1983) or the Caribbean Great Arc (e.g., Escalona & Mann, 2011). This accretion was initiated first along the Ecuadorian and Colombian western margin throughout the Late Cretaceous. During the Paleocene-Eocene, the front of the Caribbean Great Arc was already offshore western Venezuela. A significant consequence of this event is that the new accreted margin prompted the initiation of Caribbean subduction beneath NWSA (e.g., Escalona & Mann, 2011; Kroehler et al., 2011). Highly oblique subduction of the Caribbean plate below South America continued during the Paleocene and early Eocene (J. L. Pindell & Kennan, 2009). This early Caribbean subduction is associated with arc-related plutonism along the northern Central Cordillera, the lower Magdalena valley, the Santa Marta Massif and the Guajira peninsula (e.g., Bayona et al., 2012; Cardona et al., 2014; Jaramillo et al., 2017; Leal-Mejía et al., 2019) (Figure 3a). Paleomagnetic results indicate that by the middle Eocene, a kinematic change of the Caribbean plate (Boschman

Figure 3. (a) Tectonic setting of the Northwestern South American subduction zones. Main faults in the Northern Andes modified after Veloza et al. (2012); distribution of modern Volcanoes (black triangles) taken from Siebert et al. (2011); and age of the crust originated in the Nazca-Cocos spreading center (NCS) modified after Barckhausen et al. (2001), Werner et al. (2003), and Lonsdale (2005). Motion vectors relative to stable SA (Mora-Páez et al., 2019). BFS, Bocono Fault System; CC, Central Cordillera; CLIP, Caribbean Large Igneous Province; CR, Coiba ridge; CSP, Caribbean-South America-Pacific plates triple Junction; EC, Eastern Cordillera; EPR crust, East Pacific Ridge crust; GHS, Galapagos Hotspot; GUA, Guajira; LLA, Llanos basin; LMV, Lower Magdalena Valley; MB, Maracaibo Basin; MR, Malpelo Ridge; MV, Magdalena Valley; NAB, Northern Andean Block; NPDB, North Panama Deformed Belt; NCS, Nazca-Cocos Spreading center; PCA, Panama-Choco arc; PFZ, Panama Fracture Zone; RFS, Romeral Fault System; SAP, Sinu Accretionary Prism; SBFS, Santa Marta Bucaramanga Fault Zone; SJ, San Jacinto range; SM, Santander Massif; SMM, Santa Marta Massif; UFS, Uramita Fault System; YG, Yaquina graven. (b) Geological map of NWSA, modified after J. Gómez et al. (2015). Geological units: (1) Quaternary sedimentites, (2) Neogene sedimentites, (3) Neogene volcano sedimentary rocks, (4) Paleogene sedimentites, (5) Paleogene extrusive rocks, (6) Paleogene plutonic rocks, (7) Upper Cretaceous oceanic platform rocks, (8) Upper Cretaceous intrusive arc rocks, (9) Jurassic sedimentites, (10) Triassic and Jurassic metamorphic rocks, (11) Paleozoic igneous and metamorphic rocks, BF, Bucaramanga fault; GF, Garrapatas fault; IDF, Istmina deformed belt; NPDF, North Panama deformed belt; PCA, Panama-Choco arc; RFZ, Romeral fault system; UFZ, Uramita fault system.

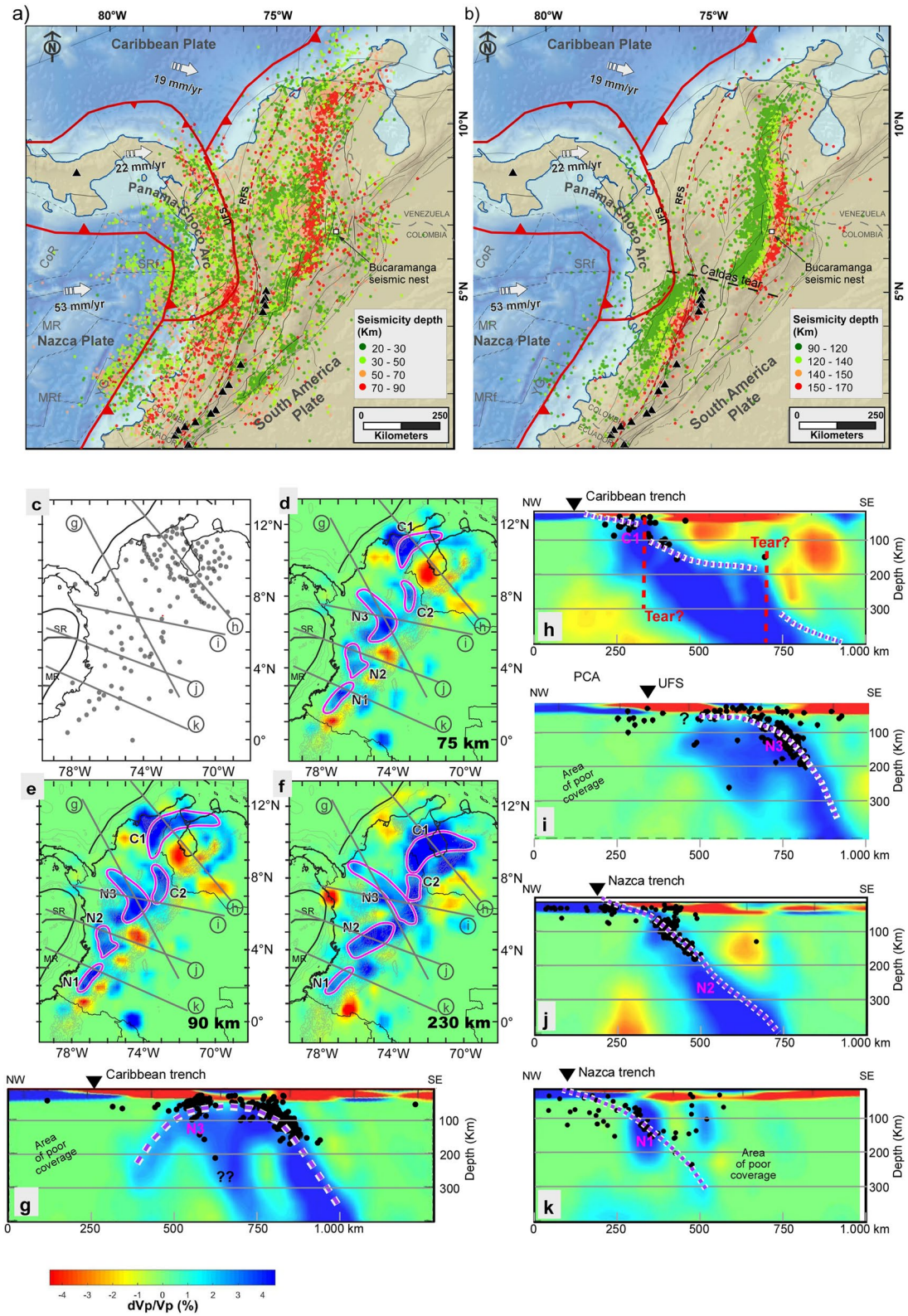

Figure 4.

et al., 2014; Müller et al., 2019; Seton et al., 2012), triggered the onset of a more orthogonal convergence and shallow subduction of the Caribbean plate beneath northern SA (e.g., Mora-Bohórquez, Oncken, et al., 2017). This change in convergence obliquity by the middle Eocene has been regarded by previous studies as the causal factor of the cessation of magmatism in northern Colombia between 56 and 45 Ma (Cardona et al., 2014) and the middle Eocene exhumation pulse in the northern central Cordillera, San Jacinto range and Santa Marta Massif (Mora-Bohórquez et al., 2018; Restrepo-Moreno et al., 2009; Villagómez et al., 2011) (Figure 3a). Additionally, the Eocene to recent eastward displacement of the Caribbean plate prompted the late Oligocene-early Miocene collision of the PCA against northern SA (Farris et al., 2011; Montes et al., 2012). Oceanic rocks accreted to SA indicate that initial collision of the PCA was located at 3°N (Duque-Caro, 1990) and then the accretion migrated northward, currently reaching as far as 8°N (Figure 3). Based on seismological and tomography interpretations, several authors have proposed that the current geometry of the Caribbean slab is characterized by shallow subduction beneath northern Colombia and western Venezuela (e.g., Cornthwaite et al., 2021; Mazuera et al., 2019; Syracuse et al., 2016; Taboada et al., 2000). Nevertheless, some previous studies suggest that flat-slab subduction may not be present in western Venezuela (Bezada et al., 2010; Sun et al., 2022).

2.2. The Northern Nazca Plate

Paleomagnetic anomalies indicate that in the past, the Colombian and Panamanian ocean-floor in the Pacific side corresponded to independent kinematic blocks known as the Coiba and Malpelo microplates (Figure 3a) (Adamek et al., 1988; Hardy, 1991; Zhang et al., 2017). However, as geodesic data (Mora-Páez et al., 2019) do not show significant current differences with the southern Nazca plate, in this paper we refer to this area, at present, as the "northern Nazca plate." As explained below, the origin of these microplates and their capture by the Nazca plate had crucial implications on the evolution of the PCA (Morell, 2015) and South American margins. For this reason, it is clear that kinematic reconstructions for the Nazca plate in southern latitudes (Figure 1) should not be used north of Ecuador. In this manuscript, we re-evaluate the kinematics of the Farallon plates and derived fragments in that region, which allows us to understand the convergence dynamics against northwestern SA.

Age dating and paleomagnetic anomalies indicate that south of 3°S, the oceanic crust originated at the East Pacific Rise (Figures 1 and 2), while the plates subducting in the Ecuadorian, Colombian, Panamanian and Costa Rican margins correspond to oceanic crust entirely formed at the combined Galapagos hotspot (GHS) track and the Nazca-Cocos spreading center (NCS, also known as the Galapagos spreading center; Figure 3a) (e.g., Lonsdale, 2005; MacMillan et al., 2004; Sallarès et al., 2003; Werner et al., 2003; Wilson & Hey, 1995). A complicated spreading history along this plate boundary determined a particular kinematics in the region (Barckhausen et al., 2001; Lonsdale, 2005). Figure 3a shows a simplified compilation of estimated ages of the ocean floor originated in the NCS (Barckhausen et al., 2001; Lonsdale, 2005; MacMillan et al., 2004; Sallarès et al., 2003; Werner et al., 2003).

While the arrangement of seafloor ages is relatively simple west of the Panama fracture zone (PFZ) (Figure 3a), with rock age increasing with distance from the NCS (Wilson & Hey, 1995), to the east of the PFZ (northern Nazca plate), the seafloor ages reveal a complex history. The youngest rocks in the northern Nazca plate (9 Ma) are located next to the eastward trending Sandra (updip extension of the Caldas tear) and Malpelo rifts (Figure 3a; we use the term rift instead of ridge for these features because these spreading axes correspond to negative reliefs or valleys) (Lonsdale, 2005). Moving away from these rifts, the seafloor becomes older until reaching the Coiba, Malpelo, and Carnegie ridges (Figure 3a), where the rocks range between 16 and 20 Ma (Barckhausen et al., 2001; Lonsdale, 2005; Sallarès et al., 2003). Furthermore, given that there is remnant seismicity associated with the Sandra and Malpelo rifts (Lonsdale, 2005), some authors have proposed that the Nazca plate in this

Figure 4. (a and b) Seismicity maps and modern volcanism in northwestern South America (NWSA). For visualization purposes, the seismic events are shown according to their depth, (a) shallower than 90 km and (b) deeper than 90 km. Earthquake data are downloaded from the catalog of the RSNC website for the period between 1993 and 2018 (https://www2.sgc.gov.co/Paginas/aplicaciones-sismos.aspx). Black triangles represent modern volcanoes taken from Siebert et al. (2011). Arrows indicate the current directions of tectonic motion according to Mora-Páez et al. (2019). Continuous gray lines correspond to main faults in the northern Andes (Modified after Veloza et al., 2012). Caldas tear lineament taken from Vargas and Mann (2013). Bucaramanga seismic nest location taken from Prieto et al. (2012). CR, Coiba Ridge; MR, Malpelo Ridge; MRf, Malpelo Rift; RFS, Romeral Fault System; UFS, Uramita Fault System; SRf, Sandra Rift; YG, Yaquina Graven. Note that north of 5°N, the seismicity is significantly reduced west of 74°W. (c–k) Tomographic model taken from Sun et al. (2022) beneath NWSA (dVp/Vp). (c) Location of seismic stations and location of cross sections. (d–f) depth slices at 75, 90, and 230 km (g–k) show tomographic cross sections. The purple lines and texts underscore well-resolve velocity anomalies interpreted in this study. Black dots in cross sections show seismicity within 10 km from the profiles.

region is fragmented into minor tectonic blocks known as the Coiba (Adamek et al., 1988; Hardy, 1991) and Malpelo (Zhang et al., 2017) microplates (Figure 3a) (we adopt this nomenclature during the Miocene).

The current Nazca slab geometry beneath SA is well constrained to the south of 5.5°N by geophysical methods (e.g., Cortés & Angelier, 2005; Syracuse et al., 2016). In this area, the termination of the northern volcanic zone (Figure 3a) (Wagner et al., 2017) and the abrupt change in the distribution of seismicity (Wadati-Benioff Zones, WBZs) have been interpreted as a slab tear (Figure 4b) (e.g., Vargas & Mann, 2013). Although a flat-slab has been considered north of this tear (e.g., Chiarabba et al., 2015; Wagner et al., 2017), the northernmost edge of the Nazca plate, and its transition between the PCA and SA is not understood. In spite of the fact that the current Nazca motion is parallel to the trench south of Panama, the presence of the South Panama Deformed Belt (SPDB, Figure 3a) has been regarded as strong evidence of oblique subduction of the Nazca plate beneath the Panama isthmus (e.g., Mann & Kolarsky, 1995; Moore et al., 1995). This is supported by young adakitic volcanism in eastern Panama that has been associated with shallow subduction of the Nazca plate (Gutscher et al., 2000). Nonetheless, Johnston and Thorkelson (1997) proposed that this adakitic signature could be the result of slab windows or localized tears in the Nazca slab that facilitated the migration of mantle melts from the lower plate.

2.3. The Northwestern South America (NWSA) Plate

The Late Cretaceous to recent geodynamics in NWSA are associated with three mountain belts developed north of 2°N, separated by along-strike topographic depressions (Figure 3a). This area is comprised by an assemblage of terranes (e.g., Cediel et al., 2003; Restrepo & Toussaint, 1988) that may be considered in terms of two broad domains separated by the Romeral fault system (RFS), which extends along the western flank of the Central Cordillera (Figure 3a). East of the RFS, the crust is constituted by a Precambrian to Paleozoic continental basement related to the Guiana Craton (Cediel et al., 2003) (Figure 3a). Conversely, west of the RFS, the crust corresponds to relict slivers of oceanic plateau rocks of the CLIP (Figure 3a) (Kerr et al., 1997; Sinton et al., 1998), accreted mostly during the Late Cretaceous to the continental Ecuadorian-Colombian margin. Nevertheless, the Gorgona and other isolated terrains in the southwestern Colombian border may have been accreted during the Cenozoic (Kerr & Tarney, 2005). In the northwest region, and bounded by the Uramita fault system (UFS; Figure 3a), the CLIP plateau rocks are replaced by intra-oceanic arc rocks that define the continuation of the Panamanian magmatic arc within SA (León et al., 2018). This terrain, known as the Panama-Choco Arc (PCA; Figure 3a) (Duque-Caro, 1990), has been interpreted as a result of a Miocene accretion event (e.g., Kellogg et al., 2019; Montes et al., 2019; J. L. Pindell & Kennan, 2009). As a result of this complex history, the northern Andean range evolved from a diachronic and heterogeneous orogenic advance (Bayona et al., 2013, 2020; Mora et al., 2010; Mora, Tesón, et al., 2020; Mora, Villagómez et al., 2020; Parra et al., 2009). The collision of the PCA against SA after the late Oligocene was a determining factor in the Andean Orogeny (e.g., Cortés & Angelier, 2005; Montes et al., 2019; Mora et al., 2015). However, the role of other driving mechanisms that controlled the mountain building in the Northern Andes, such as changes in subduction geometry and obliquity, or temporal variations in the isostatic balance has been poorly debated (e.g., Zapata et al., 2021). In this manuscript, we study the evolution of the subduction geometries and convergence angles and propose a correlation with the main orogenic episodes in the northern Andes.

3. Data and Methods

3.1. Paleo-Tectonic Reconstruction

Using the GPlates open access software v. 2.3 (Boyden et al., 2011; Müller et al., 2018; Gurnis et al., 2018; https://www.gplates.org), we modeled the relative motion of the Caribbean and Farallon/Nazca plates from 60 Ma to recent times. Our regional model was built upon the global hierarchy of plate motions and mantle reference frame proposed by Müller et al. (2019) by following the methodology of Gurnis et al. (2012) for building deforming plate boundaries through time. For visualization purposes, the South American plate was anchored and, consequently, the tectonic plate convergence velocities and obliquities presented in this paper are relative to fixed SA (the Guiana Craton) (Figures 1 and 3a). GPlates files from our paleotectonic reconstruction is included in Supporting Information S1.

Regarding the Caribbean plate kinematics, it is noteworthy that there are some differences between the motion vectors proposed by Montes et al. (2012, 2019) and other regional reconstructions such as the one proposed by Boschman et al. (2014), particularly in the time lapse Eocene-Oligocene. In Montes et al. (2012, 2019), the PCA

migrated during the Eocene-Oligocene preferentially in northerly direction, showing an important difference with respect to the leading edge of the Caribbean plate, which displaced in easterly direction during the same time span. This may have implied that the leading and trailing edges of the Caribbean plate were kinematically independent blocks, requiring lithospheric "bending" (Montes et al., 2019) or a plate boundary between them. Conversely, the reconstruction by Boschman et al. (2014), who made corrections to local block rotations for the PCA proposed in previous studies (Di Marco et al., 1995; Farris et al., 2011; Montes et al., 2012), as well as other global plate reconstructions (Müller et al., 2019; Seton et al., 2012), resolve this issue by proposing Eocene-Oligocene northeastward motion vectors for the PCA, more similar to those of the leading Caribbean plate. For that reason, we prefer to use the rotation poles of the global deforming plate model compilation of Müller et al. (2019), which includes the regional reconstruction of Boschman et al. (2014) into an optimized global reference frame, allowing us to better integrate the kinematics of the Caribbean plate, of the Farallon plate and the deformation of the northern Andes together in the most up-to-dated global compilation.

As for the Farallon/Nazca kinematics, it is important to note that rotation poles calculated for this plate in southern latitudes (motion tracks in Figure 1) (e.g., Müller et al., 2019; Pardo-Casas & Molnar, 1987) are only applicable for the Ecuadorian—Colombian offshore domain for geological times prior to the Farallon breakup (Lonsdale, 2005). Therefore, we used the rotation poles of Müller et al. (2019) for the time period between 60 and 23 Ma. For the Miocene to recent period, we used published variations in the relative positions of the NCS and the GHS (NCS and GHS in Figure 3a), as well as rates of spreading calculated from paleomagnetic anomalies (Barckhausen et al., 2001; Lonsdale, 2005; Werner et al., 2003), to propose an alternative kinematic reconstruction of the northern Nazca plate. Although there is uncertainty about the trend of the spreading centers along the already subducted slab (McGirr et al., 2020), we assume that the trend of these features in these areas does not have significant changes to those observed in the preserved area.

3.2. Upper Plate Record and Geometrical Reconstruction

A fundamental clue for reconstructing past subduction geometries is the relationship between distribution of magmatism and different parameters of subduction (Coira et al., 1982). A basic observation indicates that the presence and location of volcanic arcs are strongly dependent on the angle of subduction (Coira et al., 1982; Wagner et al., 2017). For instance, flat-slab subduction is related to continental migration of the volcanic arcs or total vanishing of magmatism (Ramos et al., 2002; Trumbull et al., 2006; Wagner et al., 2017). On the contrary, convergence obliquity seems to be not a relevant factor, as present-day volcanic arcs are found in a wide range of angles of convergence. For example, the current activity of the Sumatra volcanic arc is driven by a highly oblique subduction (Blanquat et al., 1998).

The fact that the spatial distribution of volcanism in continental margins is conditioned by the dip of the slabs, was used by Tatsumi and Eggins (1995) to state that subducting slabs are usually located at depths between 110 and 150 km below the arcs. This relationship explains why shallow subduction (where depth contours are located further from the trench) is associated with either landward migration or complete vanishing of magmatism. In this study, we use this empirical dependence to constrain the depth isocontours of subducting plates. We employ the paleogeographic reconstruction of the plate margins and the spatiotemporal distribution of Cenozoic arc magmatism. We used the recently published Cenozoic arc magmatism records along the Colombian margin (Barbosa-Espitia et al., 2019; Cardona et al., 2018; Lara et al., 2013; Leal-Mejía et al., 2019; Marín-Cerón et al., 2019; Wagner et al., 2017; Weber et al., 2020), the Ecuadorian Andes (Schütte et al., 2010) and the Panamanian isthmus (Lissinna, 2005; Montes et al., 2012; Rooney et al., 2015; Wegner et al., 2011). The resulting geometric models were integrated with published evidence of deformation in the upper plate, which allowed us to identify possible correlations between the regional plate geodynamics and first-order phases of deformation in the Northern Andes during the Cenozoic (Table S1 in Supporting Information S1). These deformation episodes are based on recently published interpretations for the Northern Andes (e.g., Bayona et al., 2013; Caballero et al., 2013; Horton et al., 2015; León et al., 2018; Montes et al., 2012; Mora, Blanco, et al., 2013; Mora, Reyes-Harker, et al., 2013; Mora et al., 2010; Mora-Bohórquez, Ibánez-Mejia, et al., 2017; Moreno et al., 2013; Pardo-Trujillo et al., 2020; Parra et al., 2009; Reyes-Harker et al., 2015; Silva et al., 2013; Villagomez & Spikings, 2013) and eastern Panama (Barat et al., 2014; Montes et al., 2012). Due to the complex interaction between the subducting Caribbean and Farallon/Nazca plates throughout the Cenozoic, the geometrical restoration of these slabs requires a three-dimensional approach. In this study, we achieved this by using the Petrel software (https://www.software.slb.com/products). The results are shown in different time-step structural contour

maps and three-dimensional diagrams. Although there is uncertainty about the actual structural evolution, we draw detailed contour maps (20 km contour interval), only for the purpose of emphasizing the geometrical changes between the different tectonic episodes.

3.3. Existing Seismological Data

In order to reconstruct the tectonic evolution in the area, we defined the main observables of the present-day configuration of subducting fragments beneath NWSA. To accomplish that, we used published seismicity data and a recent tomographic model. The seismicity data set comprises a catalog of 177,000 seismic events (magnitude < 6.8) during the period 2003–2018 taken from the National Seismological Network of Colombia (RSNC; Figures 4a and 4b). The tomographic data that we used correspond to the recently published finite-frequency velocity model for the Northern Andean region developed by Sun et al. (2022) (Figures 4c–4k). In that tomography they obtained a P wave velocity model based on seismic events retrieved from 165 stations in Colombia and 65 stations in Venezuela (Sun et al., 2022). We used the *dVp*/*Vp* anomalies, which according to Sun et al. (2022) provide a reliable resolution for interpreting regional and continuous high-velocity anomalies that could be related to distinct slab segments.

3.3.1. The Nazca Slab South of 5.5°N

From geophysical data, the most striking feature in the deep tectonics beneath northwestern SA is the offset in the WBZ (Figure 4b) at 5.5°N known as the Caldas tear (Vargas & Mann, 2013). This abrupt change in seismicity coincides with a change in the tomographic model (Figures 4d–e, 4f) and with the northern boundary of the Northern Andean arc, which is continuous to the south of this location (Pennington, 1981; Vargas & Mann, 2013; Wagner et al., 2017) (Figures 2 and 3). The dashed lines in Figure 4 define the boundary of the largest high-velocity anomalies (blue color) that can be correlated with cooler and denser subducting slabs. The tomographic cross section j in Figure 4 suggests that the Nazca plate south of the Caldas tear is steeply subducting. Some authors (Sun et al., 2022; Vargas & Mann, 2013) have identified a velocity discontinuity at 3°N (Figures 4d–4f). However, as the cross-section k and seismicity data (Figure 4b) are not clear indicators of change in geometry, it could be related to a thermal perturbation in the subducting slab.

3.3.2. The Caribbean Slab North of 8°N

To the north of the Caldas tear, the most evident feature is the continuous northward trend of intermediate-depth seismicity that defines a WBZ running from 5°N to 10°N, at about 73°W (Figure 4b). The subducted slab north of 8°N is clearly part of the Caribbean plate, since this segment is in close proximity to the Caribbean trench (e.g., Cornthwaite et al., 2021; Sun et al., 2022). Seismicity and tomographic imaging to the west of the high seismicity zone indicate that the Caribbean plate is shallowly subducting in this area (Figure 4). Mazuera et al. (2019) interpret that the Caribbean plate continues shallowly subducting as a single slab beneath northwestern Venezuela. However, in the model of Mazuera et al. (2019), the tomographic model is restricted to the upper 60 km. Nevertheless, the high seismicity zone (WBZ) with events between 90 and 160 km at about 73.5°W (Figure 4b) indicates that the subducting Caribbean slab is sinking beneath the Eastern Cordillera in eastward direction (Vargas & Mann, 2013), which is not consistent with flat-slab subduction east of the WBZ. Additionally, we prefer the interpretation of no-shallow subduction beneath northwestern Venezuela because it is in agreement with the tomographic model (Figure 4h), that show that the Caribbean configuration changes east of 73.5°W. At that position, the tomographic slices (Figures 4d–4f) do not show a clear surface continuity of the Caribbean slab as a single segment (Bezada et al., 2010, and references therein).

3.3.3. Slab Segments Between 5.5°N and 8°N

Although the continuity of intermediate-depth seismicity running from 5.5°N to 10°N (Figure 4b) can be interpreted as Caribbean slab subduction (e.g., Bernal-Olaya et al., 2015; Sun et al., 2022; Taboada et al., 2000), a puzzling fact is the coincidence between the southern end of this trend and the Caldas tear at 5.5°N, interpreted as a rupture in the Nazca plate (Vargas & Mann, 2013). The fact that the tomographic anomalies are diffuse in this area and allow different interpretations (Bernal-Olaya et al., 2015; Sun et al., 2022; Taboada et al., 2000; Vargas & Mann, 2013) is the main reason for the lack of agreement on a definitive tectonic model. In this sense, tomography models have shown not to be conclusive to determine the southern edge of the Caribbean slab and the northern edge of the Nazca slab. Or even, it is possible that there is an area of overlapping north of the Caldas tear (Sun et al., 2022).

Interestingly, there is a complex pattern of high velocity anomalies north of the Caldas tear that runs in a different direction than the regional trend (anomaly N3 of Figures 4d–4f). This pattern defines a parabolic shape in the cross-section g of Figure 4 that could be regarded as a geophysical artifact. Considering that similar patterns have been identified in different tomographic studies in this area, at depths below 50 km (Bernal-Olaya et al., 2015; Sun et al., 2022; Syracuse et al., 2016; Yarce et al., 2014), we ruled out this anomaly as a geophysical artifact. We consider that this pattern could be related to a subducting slab fragment north of 5.5°N that seems to be bending east of the CSP triple junction.

4. Results

4.1. Plate Kinematic Reconstruction

Below, we integrate the results of our kinematic reconstruction of the Northern Nazca plate (Figure 5) and Southwestern Caribbean plate (Figure 6) with a compilation of observations made by different authors.

4.1.1. Nazca Plate Reconstruction

Previous studies have concluded that the Farallon kinematics were relatively homogeneous during the Paleogene (Figures 1 and 5f) (e.g., Müller et al., 2019). However, by the late Oligocene, the GHS got aligned with a preexisting fractured or weakened zone, triggering the Farallon plate breakup and the origin of the Nazca and Cocos plates at 23 Ma (Figure 5a) (Lonsdale, 2005). The initial oceanic spreading along the new Nazca-Cocos plate boundary prompted a differential direction of displacement for the Nazca and Cocos plates, representing a more orthogonal convergence against Central and SA (Figure 5a). This motion pattern changed at around 18 Ma, when the spreading center jumped to a more southern position (note shift in spreading-axis position between Figures 5a and 5b) (Barckhausen et al., 2001; Werner et al., 2003). From a kinematic point of view, this E-W divergent plate boundary was separating an easterly motion for the Nazca plate, and a more northerly motion for the northern segment, that included the Cocos plate and the proto-Coiba and proto-Malpelo microplates (Figure 5f), which were obliquely subducting beneath SA. After 15 Ma, the spreading axis in the easternmost Pacific shifted to the Malpelo rift (Figure 5b) and shortly after, but with concurrent activity, to the Sandra rift (Figure 5c) (Lonsdale, 2005). This complex oceanic spreading generated a northward motion to the north of the Malpelo spreading center (Figure 5c). Finally, the spreading along the Sandra and Malpelo rifts abruptly ended at 9 Ma, and as a consequence, the Coiba (CM) and Malpelo (MM) microplates became part of the Nazca plate (Figure 5d) (Lonsdale, 2005; Sallarès et al., 2003), leading to the establishment of a transform fault boundary between the Cocos and Nazca plates (the PFZ, Figure 3a) (Lonsdale, 2005; Morell, 2015; Sallarès et al., 2003). As a consequence of this late Miocene coupling of the Coiba and Malpelo microplates to the Nazca plate, the convergence direction became more oblique against the Panama isthmus (Morell, 2015; Rooney et al., 2015) and more orthogonal against the northern South American margin (Figures 5d and 5e). In other words, the modern Nazca-Cocos plate boundary and the current tectonic configuration in the Pacific, offshore Colombia and Panamá, were established after 9 Ma.

4.1.2. Southwestern Caribbean Plate Reconstruction

According to the reconstructions of Boschman et al. (2014), Müller et al. (2019) and this study, the PCA was located about 1,000 km in a southwestern position of its current location during the Paleocene (60 Ma) (Figures 3a and 6b) and was moving toward the NE, defining a highly oblique convergence with the South American margin (Figure 6b). During the Paleocene, the Farallon plate margin, defined by its boundary with the Caribbean plate to the northwest and the South American plate to the southeast, formed a subtle curved trend (Figure 6b). Throughout the Paleocene-early Eocene, the southwestern Caribbean plate continued moving in SW-NE direction at an average speed of 36 mm/yr (Figure 6a) (Boschman et al., 2014; Müller et al., 2019). During the middle Eocene, there was an abrupt shift toward the SE (Boschman et al., 2014; Müller et al., 2019) (Figure 6d), that implied a more orthogonal convergence direction against SA. As a result, the CSP triple junction moved northeastward during the Eocene and the vertical-axis curvature between the Farallon-Caribbean and Farallon-Peruvian trenches significantly increased to become almost orthogonal (Figures 6c and 6h).

During the late Eocene-Oligocene, the Caribbean plate continued moving in an eastward direction (Boschman et al., 2014; Müller et al., 2019) at an average rate of 22 mm/yr (Figures 6d and 6e), moving the PCA toward the Colombian margin (Figure 6d). At ca. 23 Ma, the eastward motion of the Caribbean plate culminated in the onset of collision of the intra-oceanic PCA against the Colombian margin at about 300 km to the south of the present-day CSP triple junction (Figure 6e) (Duque-Caro, 1990). Although the Caribbean kinematics during

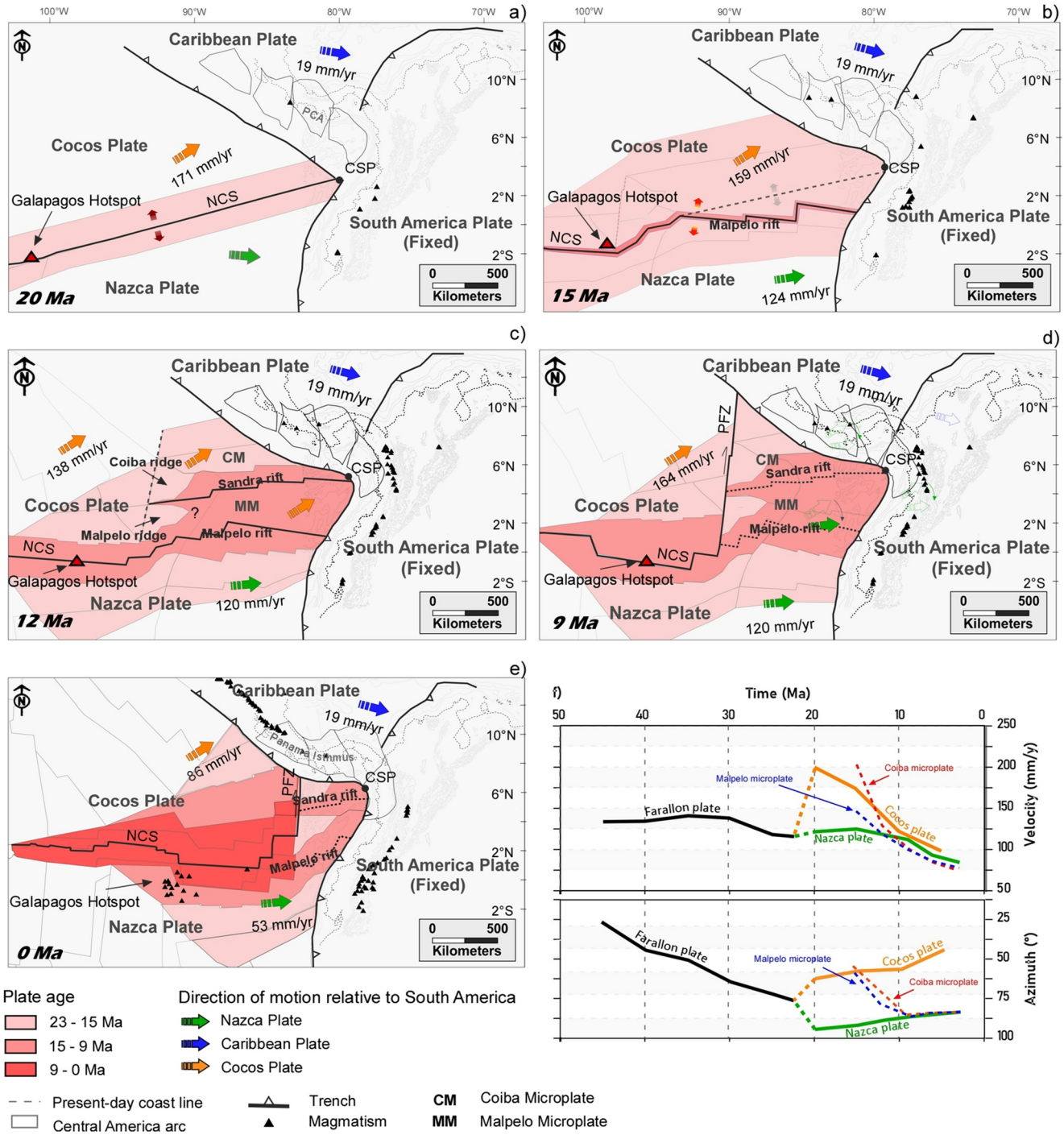

Figure 5. (a–e) Paleotectonic reconstruction of the Nazca-Cocos plate boundary (NCS) from the early Miocene to the present-day. Red colors indicate the age of the ocean-floor according to previous paleomagnetic studies (Barckhausen et al., 2001; Lonsdale, 2005; MacMillan et al., 2004; Werner et al., 2003). (f) Estimated evolution of the motion direction and velocity of the Farallon, Nazca and Cocos plates, and the Coiba and Malpelo microplates relative to stable South America.

the Miocene, after initial collision, were dominated by eastward plate motion, the northeasterly pushing of the subducting Farallon plate, as well as the resulting arc fragmentation and rotation of blocks (Farris et al., 2011; Montes et al., 2012, 2019) caused the continued northward migration of the accretion front against SA (Figures 6f and 6g).

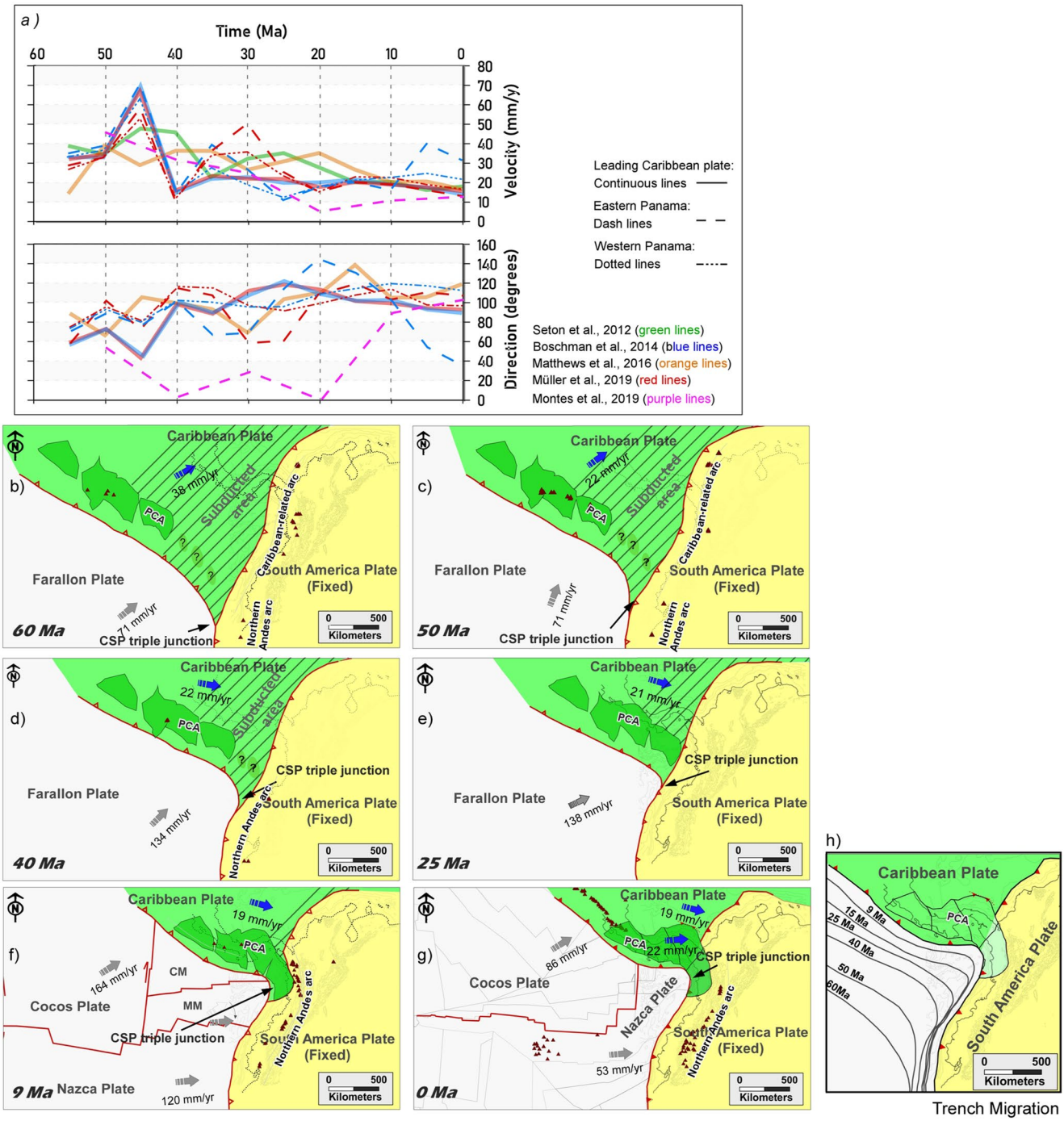

Figure 6. (a) Comparison of different plate motion vectors of the Caribbean plate (leading Caribbean plate, eastern Panama and western Panama) relative to stable South America according to several authors (Boschman et al., 2014; Matthews et al., 2016; Montes et al., 2019; Müller et al., 2019; Seton et al., 2012). (b–g) Paleotectonic reconstruction of the southwestern Caribbean plate motion throughout the Cenozoic showing the migration and convergence of the PCA against SA. Note that, as a consequence of the Caribbean kinematics, the CSP triple junction migrated in northward direction. (h) Migration of the Caribbean-Pacific trench. CM, Coiba microplate; LMV, Lower Magdalena Valley; MM, Malpelo microplate; PCA, Panama-Choco arc; SA, South America. (h) Trench position at the CSP triple junction at different time steps during the Cenozoic.

5. Discussion

By using the reviewed kinematics of the subducting plates, along with several lines of evidence on the upper plate, we made a reconstruction of the subducting geometries. The challenge to accomplish this reconstruction is

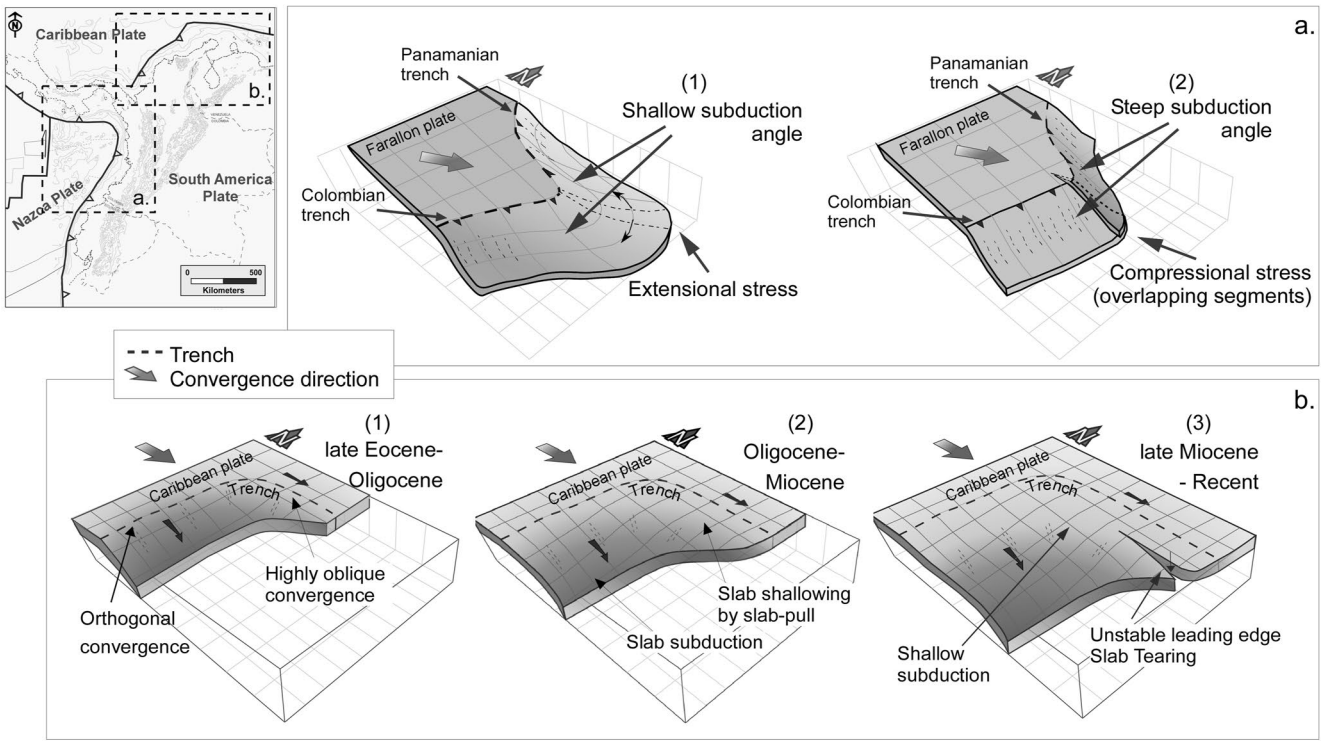

Figure 7. Conceptual models used to reconstruct the evolution of subducting geometries beneath northwestern South America. (a) Simplified sketch showing two end-member scenarios for the subduction geometry of a single slab obliquely subducting under two orthogonal margins, similar to the Farallon subduction at the transition between the Panama-Choco arc (PCA) and South America. In (a1), it is assumed that slab subduction is accommodated by reducing the angle of subduction at the inflexion point, favoring the slab flattening on both margins. It is important to note that the continued subduction progressively increases the extensional stress behind the hinge zone, which could lead to slab rupture at advanced stages of flattening. In (a2), it is assumed that the slabs subduct with steep angles on both margins, prompting the compressional stress behind the trench due to a reduced accommodation space. (b) Simplified sketch showing three time-steps of the convergence of the Caribbean plate against northwestern South America (in this sketch the effect of the PCA accretion is not considered). Given the curved trench geometry and the direction of convergence, the southernmost segment is characterized by orthogonal subduction, while the northeastern segment by a highly oblique convergence. Although this configuration is similar to other models that account for Subduction-Transform Edge Propagators (STEP faults) (Govers & Wortel, 2005), the very slow convergence could inhibit the faulting and favor the slab shallowing near the oblique margin. We consider that this is the case in the area shown in (b1), as the low convergence rate of the Caribbean plate, in combination with the margin shape induced the flat-slab subduction by slab-pull from the northeastern side of the margin (b2). At advanced stages, the cumulative shallow subduction may not be sustainable, which may prompt the faulting in the leading edge of the slab (b3).

that the heterogeneous margin and variable convergent obliquity through time demand a three-dimensional analysis. Figure 7 shows the conceptual models that were used to reconstruct the geometrical evolution of the slabs.

5.1. Farallon/Nazca Plate Geodynamics

The evolution of the Farallon/Nazca plate convergence against the NWSA can be divided into three major episodes separated by the breakup of the Farallon plate during the late Oligocene and the establishment of the modern northern Nazca plate kinematics during the late Miocene.

5.1.1. Paleocene to Late Oligocene (65–23 Ma)

The continuity of the Farallon slab to the northeast of the South American margin is critical for understanding the geodynamics prior to the Farallon breakup. However, geophysical methods do not allow a clear definition of this transition (e.g., Wagner et al., 2017). For this reason, previous models (e.g., Taboada et al., 2000; Vargas & Mann, 2013) have not interpreted the continuity of the subducting Farallon/Nazca plate between the South American margin and the PCA. On the contrary, below we argue that the Farallon plate evolved almost as a continuous slab segment, conditioning the geodynamics at the triple-junction.

According to Müller et al. (2019) and this reconstruction, during the Paleogene, the Farallon kinematics (Figures 1 and 5f) defined an oblique convergence against the PCA and South American margins. Although the oceanic crust of the Caribbean plate east of the PCA during the Paleocene is already subducted under the

South American margin (see subducted area in Figure 6a), the most likely geometrical interpretation is that the trench followed a continuous trend, linking the PCA and South American trenches during the Paleocene (Figure 6a). This is supported by the spatiotemporal distribution of magmatism along the PCA and South American margins (Timbiqui arc in southernmost Colombia and Ecuador) (Barbosa-Espitia et al., 2019; Grajales et al., 2020) during the Paleogene-Eocene which can be regarded as Farallon-related arc (at this point we are not evaluating the Caribbean-related arc in northern Colombia) (Figures 8a and 8b) (e.g., Cardona et al., 2018; Leal-Mejía et al., 2019; Wegner et al., 2011). The Paleocene configuration of the Farallon margin defined a lateral transition between ocean-continent (SA) and ocean-ocean (Caribbean) subduction that, in agreement with Cardona et al. (2018), resembled an Aleutian type margin (Figure 8a). Cardona et al. (2018) and Barbosa-Espitia et al. (2019) provide geochemical evidence of this magmatic transition. Assuming these intrusions occurred at a depth between 100 and 150 km, similar to the present-day volcanic zone, the Farallon plate was subducting below the margin at a steep angle (>25° dip) during the Paleocene (green contour lines on Figure 8a).

This configuration changed during the middle-late Eocene (Figures 8b and 8c) when the curvature of the Farallon trench strongly increased at the CSP triple junction, shaping a nearly orthogonal corner (green contour lines on Figure 8c). The coincidence between this trench constriction and the contemporaneous decrease in the Farallon-related magmatism activity throughout the late Eocene-Oligocene on the northern South American margin (Bayona et al., 2012; Leal-Mejía et al., 2019) and the eastern PCA (Figures 8c and 8d) (Lissinna, 2005; Wegner et al., 2011) suggests that the slab segments beneath these margins may have formed a continuous subduction system.

We propose that depending on the angle of subduction, there are two possible end-member scenarios for the subducting slab geometry beneath the PCA and SA margins from the late Eocene (Figure 7a). Considering that the Farallon plate evolved as a single subducting element implies that the slab bent tightly to the east of the CSP triple junction. This leads to an accommodation-space problem in the hinge zone that causes trench-parallel shortening strain in the bent slab, resulting either in subsequent rupture and overlapping of slab segments (Figure 7a2) or in a reduced subduction angle with a regional flat-slab around the hinge zone (Figure 7a1). A similar flat-slab setting associated with a convergent triple junction has been reported beneath Japan (Faccenna et al., 2018).

By 60 Ma, the area of influence of the Farallon plate subduction was restricted to latitudes more southerly than Colombia (Figure 8a); however, the northward migration of the triple junction during the Paleocene progressively increased the role of this plate on the tectonics of northwestern SA (Figures 8b–8d). We consider that between late Eocene and late Oligocene time, flat-slab subduction of the Farallon slab behind the triple junction is the most likely scenario (Figure 7a1). This is suggested by the fact that the deformation migrated toward the backarc region, with associated onset of inversion of rift structures in the Eastern Cordillera of Colombia (Table S1 in Supporting Information S1) (e.g., De la Parra et al., 2015; E. A. Gómez et al., 2003; Martinez et al., 2022; Mora et al., 2010; Mora, Reyes-Harker, et al., 2013; Mora, Blanco, et al., 2013; Parra et al., 2009; Rosero et al., 2022; Sánchez et al., 2012; Saylor et al., 2012), coinciding with a deformation phase in eastern Panama (Barat et al., 2014; Montes et al., 2012). This interpretation is additionally supported by the reduction in Farallon-related magmatism activity throughout the late Eocene-Oligocene on both the PCA and SA margins (Leal-Mejía et al., 2019; Wegner et al., 2011). Nevertheless, although not indispensable, shallow subduction could also be associated with landward migration of magmatism (Trumbull et al., 2006), which could support the hypotheses by Bayona et al. (2012), who propose that there was volcanic activity in the Eastern Cordillera during the Eocene. Though detrital grains back up this interpretation, these intrusive bodies have not been found yet. Apart from that, the Oligocene magmatic quiescence in southern Colombia-Ecuador may have required an additional unknown factor, or alternatively, a slab flattening of greater wave amplitude than that illustrated in Figure 8d may have occurred. To conclude this section, the approximate simultaneity of events in the area of influence of the Farallon plate subduction in both the PCA and South American margins suggests that these subduction zones did not evolve independently, but rather as a single system shallowly subducting.

The approximate simultaneity of decreased magmatic activity during the late Eocene-Oligocene (Figures 8c and 8d) on both the PCA and SA margins (Barbosa-Espitia et al., 2019; Cardona et al., 2018; Leal-Mejía et al., 2019; Wegner et al., 2011) suggests that the subduction zones along these margins did not evolve independently. Instead, the Farallon plate subducted as a single slab beneath these margins during the Oligocene, favoring the flat-slab model proposed in Figure 7a1.

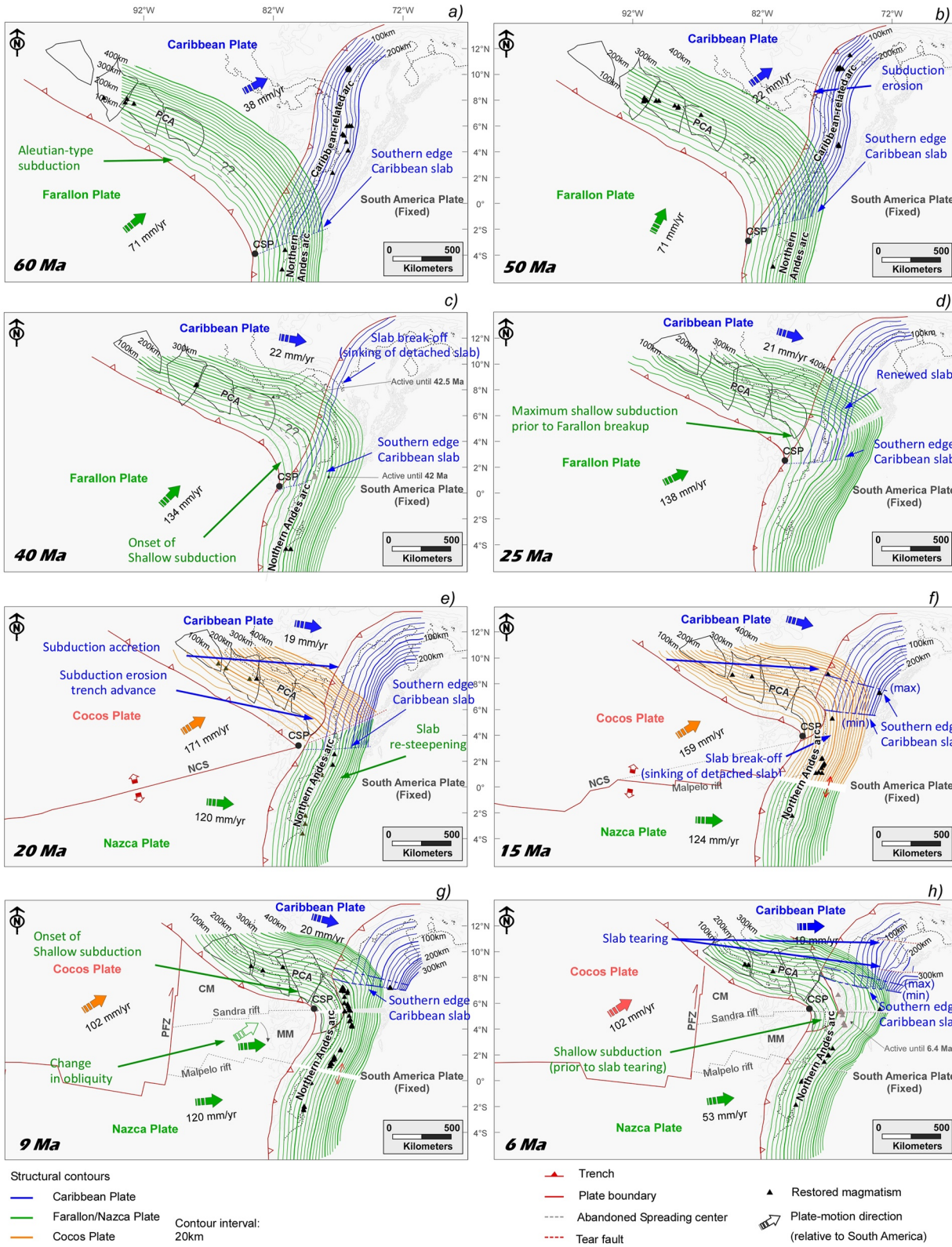

Figure 8.

5.1.2. Early to Latest Middle Miocene (23–9 Ma)

The Oligocene flat-slab subduction during the Oligocene is in line with the hypothesis formulated by Lonsdale (2005), who suggests that the stress that broke the Farallon plate was the result of slab pull forces from the Panamanian and Colombian margins, being coherent with the extensional pull between the Central and South American subduction zones (as conceptualized in Figure 7a1) and the alignment of this weakness zone with the GHS by the early Miocene (Figure 5a). Nevertheless, there is no evidence in the South American margin of this breakup and subduction of the initial spreading center during the early Miocene (approximately in a NE of the Istmina deformed belt). A similar configuration is found today in the southern Andes at 46°S, where the Nazca-Antarctic plate boundary, which is an active spreading ridge, subducts beneath SA (Bourgois et al., 2016). This subduction setting in Patagonia prompts a particular volcanism enriched in mantle fluids in the arc position (Guivel et al., 2003). On the contrary, the lack of late Oligocene volcanism on the northwestern South American margin, over the subducted Nazca-Cocos plate boundary (a spreading center) can be explained by the fact that during the Oligocene-Miocene, the subducted zone of initial rupture (Figure 7a1) was overlapped by the subducting Caribbean slab (Figure 8e), implying that the Caribbean plate must have acted as a blanket that inhibited the rise of magmatic fluids to the South American plate. This interpretation is different from that of McGirr et al. (2020), who consider the Azuero zone in Panama as the initial rupture point of the Farallón plate. However, if that scenario were correct, a magmatic record associated with the initial crustal spreading would indeed be in that region.

Interestingly, subduction-related magmatism renewed during the late Oligocene in the PCA and SA (Figure 8e) (Leal-Mejía et al., 2019; Marín-Cerón et al., 2019; Wagner et al., 2017; Wegner et al., 2011), suggesting a re-steepening of the now separated Nazca and Cocos plates in the Panamanian and Colombian margins. Despite the change in slab dip, the deformation record in SA continued without significant acceleration or deceleration in the late Oligocene (Mora, Villagómez et al., 2020; Villagómez et al., 2011), perhaps because the impact due to slab steepening was compensated by the change in convergence obliquity that followed the Farallon breakup (Figures 8d and 8e).

This steepening, and the increasing curvature of the trenches at the CSP triple junction (Figure 8e), probably resulted in a zone of compressive stress in the subducting slab at the inflection junction (Figure 7a2), indicating an evolution from the model shown in Figure 7a1 to the model shown in Figure 7a2 during the early Miocene. The new compressive stress in the inflection point may have prevented the oceanic spreading along the original rupture zone (Figure 5a), forcing a southward jump of the ridge-transform system by 18 and 15 Ma (Figure 5b) (Barckhausen et al., 2001; Werner et al., 2003). This gave way to the Sandra and Malpelo rifts, and in turn to the Coiba and Malpelo microplates during the early-middle Miocene (Figures 5b, 5c, and 7f). These jumps in the ridge-transform system (Barckhausen et al., 2001; Werner et al., 2003) are also described by McGirr et al. (2020), however, their model keeps the main crustal spreading close to the original axis, which difficult the development of the Coiba and Malpelo microplates during the middle Miocene. Note that these microplates stopped growing after 9 Ma.

From a kinematic point of view, the Sandra and Malpelo spreading centers imprinted a northward component of motion to the Coiba and Malpelo microplates. As a result, the plate beneath NWSA and the Panamá isthmus had a Cocos-like motion during most of the early-middle Miocene, implying an orthogonal convergence against the Panama isthmus (Morell, 2015; Rooney et al., 2015) and an oblique convergence against SA (Figure 8f). This interpretation, however, differs from the model by McGirr et al. (2020), who assume that the Sandra and Malpelo rifts did not project eastward beneath SA due to flat-slab subduction to the east. Nonetheless, the onset of flat-slab subduction at this latitude took place during the late Miocene (Chiarabba et al., 2015; Wagner et al., 2017).

While the moderate exhumation rates reported in the northern Andes throughout the early-middle Miocene (Table S1 in Supporting Information S1) (Mora, Villagómez et al., 2020) is consistent with the continued oblique convergence during most of that time span (Figure 8f), the accelerated Andean deformation during the late

Figure 8. (a–h) Suggested reconstruction of the northwestern South America (SA) and Panama subduction systems considering the paleotectonic reconstructions (Figures 5 and 6), the restored development of magmatism, the change in the geometry of the plate boundaries and other concepts discussed in this paper (Figure 7). Farallon/Nazca (green), Cocos (green), and Caribbean (blue) slabs. Black triangles show paleoactive magmatism. Big arrows indicate the direction of plate motion relative to stable SA. Blue dashed lines show the suggested alternatives for the southern boundary of the Caribbean plate, minimum resulting from the development of magmatism east of the Panama-Choco arc (PCA), and maximum derived from the Caribbean kinematics after initial contact between the PCA and SA. Light dotted line shows the present-day coastal line. Note that the purpose of showing this relatively detailed interpretation (contour interval 20 km) is to emphasize the geometric changes between the different tectonic episodes.

Miocene could be associated with the attachment of the Coiba and Malpelo microplates by the Nazca plate. Morell (2015) and Rooney et al. (2015) recognize the implications of this tectonic event in the Central American tectonic history.

5.1.3. Late Miocene to Recent (9–0 Ma)

The kinematic change at 9 Ma due to the attachment of the Coiba and Malpelo microplates to the Nazca plate represented a major tectonic event that modified the convergence directions and the subduction system beneath Eastern Panama (Morell, 2015) and Northern SA. The eastward migration of the arc-related magmatism in the Central Cordillera of Colombia during the Miocene (Figures 8e–8h) (Leal-Mejía et al., 2019; Marín-Cerón et al., 2019; Wagner et al., 2017) has been associated with a progressive shallowing of the Nazca slab (Wagner et al., 2017). Particularly, the magmatic migration north of 5.5°N (Figure 8g) that initiated the volcanism in the Eastern Cordillera at 6 Ma (Bernet et al., 2016; Pardo et al., 2005), supports a shallow subduction of the Nazca plate during the late Miocene (Figure 8h) (Chiarabba et al., 2015; Wagner et al., 2017). However, the uninterrupted magmatism in the South American arc south of 3°N (Figures 8g and 9a) indicates that the late Miocene shallow subduction was operating only in the most northern Nazca slab segment, but not in southern latitudes. The change in convergence direction, in combination with the already subducted slab beneath Panama, and the complicated subduction geometry east of the CSP triple junction (Figure 8g), very likely triggered this new phase of flattening behind the triple junction during the late Miocene (Figures 7a1, 8g, and 8h). Therefore, this mechanism of slab flattening supports a Nazca plate behaving as a single subduction system beneath the Eastern Panama units (Gutscher et al., 2000) and the Northern Andes.

Nonetheless, while there is agreement of late Miocene to recent flat-slab subduction of the Nazca plate north of 5.5°N in SA, on the Panamanian side there is controversy on the presence (Gutscher et al., 2000) or absence of the Nazca plate (e.g., Johnston & Thorkelson, 1997). Even though previous studies do not interpret the continuity of the Nazca plate beneath Central and SA, our reconstruction suggests that this plate is continuous east of the CPS triple junction, connecting both margins by means of a flat slab. Moreover, though the present-day northward motion of the Nazca plate beneath Panama is minimal, the amount of crust subducted before 9 Ma in northward direction was significantly more important (see white contours in Figure 8), which weakens the model of a slab window beneath Panama (Johnston & Thorkelson, 1997; McGirr et al., 2020).

It is very likely that the change in convergence obliquity, and the flat-slab subduction of the northern Nazca plate during the late Miocene (Figures 8h and 9a) played a major role in the onset of accelerated deformation and the main phase of Andean orogeny (e.g., Parra et al., 2009; Mora et al., 2006, 2010; Mora, Tesón, et al., 2020; Mora, Villagómez et al., 2020; Carrillo et al., 2016) (Table S1 in Supporting Information S1). During the late Pliocene, the renewed volcanism in the Central Cordillera south of 5.5°N indicates steepening of the Nazca slab after its tearing (Caldas tear) and separation from the northern segment that stayed flattened (Figure 9a) (Wagner et al., 2017). As the geometrical conditions shown in Figure 7a1 prevailed only in the northernmost segment, the slab steepening was induced merely in the southern segment (Figure 8h), triggering the modern volcanism south of 5.5°N (Figure 9a) (Leal-Mejía et al., 2019; Marín-Cerón et al., 2019; Vargas & Mann, 2013; Wagner et al., 2017).

5.2. Caribbean Plate Geodynamics

The convergent geodynamics of the Caribbean plate against NWSA were dominated by two events during the Cenozoic: the abrupt kinematic change during the middle Eocene and the accretion of the PCA to SA.

5.2.1. Kinematic Change During the Middle Eocene

Previous studies agree that the front of the Caribbean Great Arc during the Paleocene-Eocene was located offshore western Venezuela (Escalona & Mann, 2011; J. L. Pindell & Kennan, 2009). Therefore, the presence of arc-related volcanism in the Colombian margin during the Paleocene-early Eocene (Antioquia, Lower Magdalena valley, Santa Marta, Guajira) indicates that the Caribbean plate was already subducting with a high angle of obliquity beneath the NWSA (Figures 8a and 8b) (Bayona et al., 2012; Cardona et al., 2011; Jaramillo et al., 2017; Leal-Mejía et al., 2019). Although there is consensus that the entire Caribbean plate shifted from northeastward to eastward migration during the middle Eocene (Figures 6a and 6d) (Matthews et al., 2016; Müller et al., 2019; Seton et al., 2012), the implications on the convergence with SA are not well understood. Several authors propose

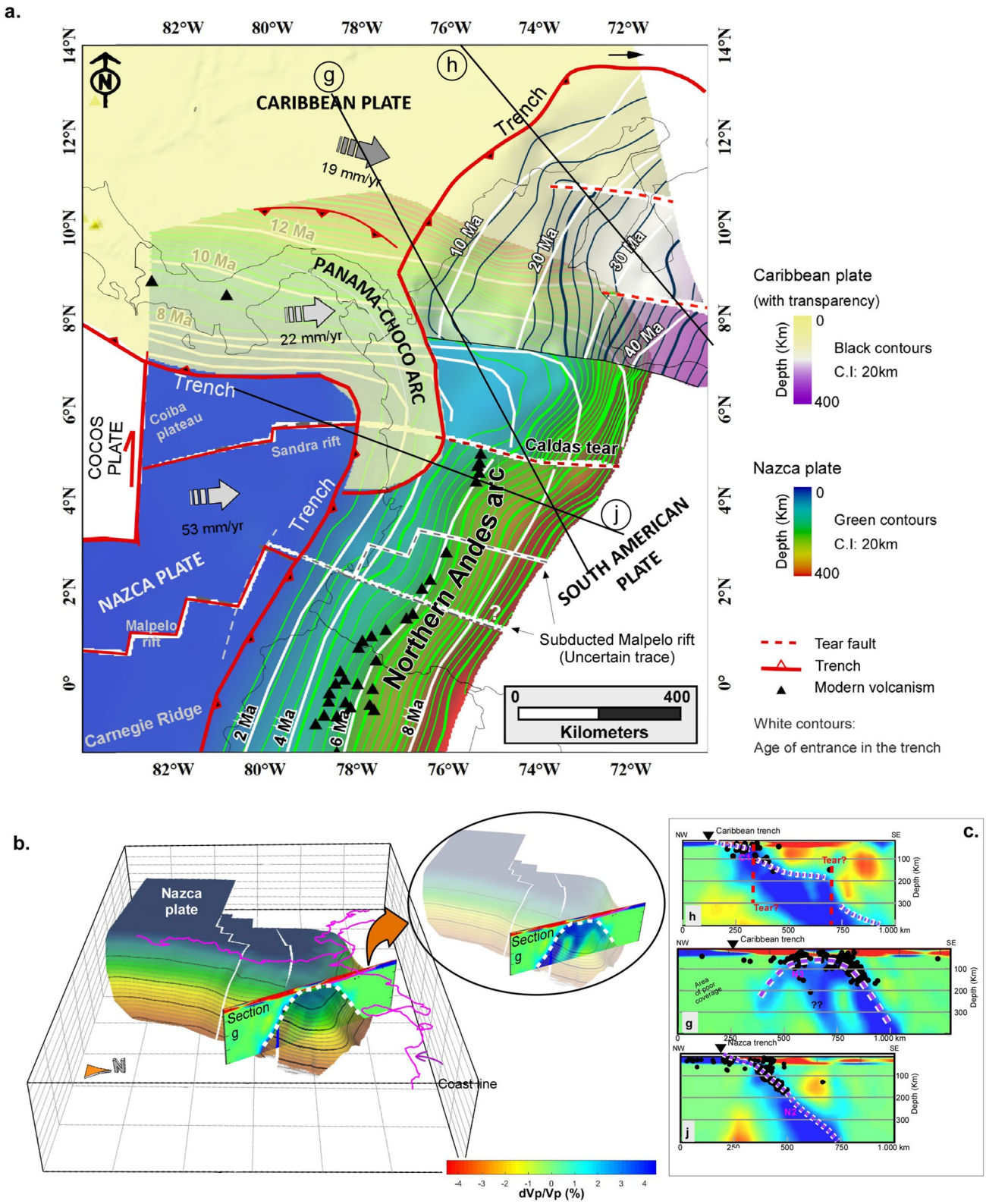

Figure 9.

that this kinematic change coincided in time with the initial subduction of a thicker lithosphere and extinction of Caribbean-related magmatism, which defined the onset of flat-slab subduction of the Caribbean plate (Bayona et al., 2012; Cardona et al., 2011). The influence of the slab thickness on the subduction geometry, however, was not evaluated in our kinematic model. Apart from that, below we propose that the Eocene change in convergence obliquity was associated with a breakoff in the Caribbean slab.

Although the distribution of arc-related magmatism suggests at least 300 km of subducted Caribbean slab before the middle Eocene (Figures 8a and 8b), an implication of this protracted obliquity is that the slab may have been unstable due to its negligible downward (eastward) motion. We speculate that the abrupt change in Caribbean plate convergence, that became more orthogonal by the middle Eocene (Figures 6c and 6d) (Boschman et al., 2014; Müller et al., 2019), may have led to the breakoff and collapse of this nearly stagnant slab segment (Figure 8c). Experimental analyses by Andrić-Tomašević et al. (2023) indicate that long-term oblique ocean-continent subduction is sufficient to trigger slab tearing (breakoff), which may be reinforced by changes in convergence obliquity or velocity. Additionally, subduction of the thicker Caribbean slab by the Eocene (Bayona et al., 2012) may also have been a factor of rupture. The detached segment, however, must have been sunk into the mantle, as suggested by experimental analyses on similar kind of settings (Duretz et al., 2011), accounting for the lack of evidence on the tomography. This slab breakoff is supported by the paradoxical cessation of magmatism when the Caribbean convergence became orthogonal after the middle Eocene (Figures 8c and 8d).

Another implication of the new Caribbean kinematics after the middle Eocene (Figure 8c) is that since that moment, the margin laterally transitioned between an orthogonal subduction to a highly oblique against NWSA (Figure 7b1). This geometric configuration may prompt the formation of subduction-transform edge propagators (STEP faults) (Govers & Wortel, 2005; Mora-Bohórquez, et al., 2017b), however, under low convergence rates, the slab could not be torn apart in the transform margin, which would result in shallow subduction by slab-pulling (Figure 7b2) (Govers & Wortel, 2005). We consider that this was the case in northern SA, where the shape of the continental margin, and the direction of motion (Figure 6a), may have forced the shallow subduction of the Caribbean plate since the middle Eocene (Figures 7b2 and 8c). The previous breakoff of the slab and the buoyant nature of this lithosphere (Bayona et al., 2012; J. Pindell et al., 2005) may have favored this process.

5.2.2. Accretion of the Panama-Choco Arc (PCA) to NWSA

Though the accretion of the PCA to SA is widely mentioned in the literature (e.g., Duque-Caro, 1990; Montes et al., 2012), the geodynamic mechanism of this event is not understood. Most previous interpretations agree that the Caribbean plate is subducting east of the PCA (Figure S3 in Supporting Information S1) (e.g., Kellogg et al., 2019; Vargas & Mann, 2013). However, in the following lines we explain why our preferred interpretation is that there is no Caribbean slab east of the PCA (Figure 8f).

The initial point of contact of the PCA against SA was approximately 400 km to the south of the present Panama Isthmus during the late Oligocene (Figures 10a–10c). However, during the early and middle Miocene, the PCA was virtually forced into the continent, defining a concave suture (Figure 10a). The paleogeographic reconstruction (Figure 10) indicates that the deformation was not symmetrical on both sides of the suture after first contact of the PCA with SA. On the one hand, the compressive strain fragmented the PCA and rotated the resulting blocks forming an orocline (Montes et al., 2012), the northeastward advance of the southern edge of the Caribbean plate, and the northward migration of the accretion front against SA. It is very likely that this behavior was prompted by the northeastward pushing of Farallon-derived plates (Figures 5d–5f and 10a–10c). On the other hand, the most important change on the continental side was the eastward advance of the margin by at least 200 km (Figure 10). In spite of this trench advance, several recent studies indicate that deformation and exhumation rates were not significantly increased in the northern Andes during the early-middle Miocene (Mora, Villagómez et al., 2020; Pérez-Consuegra et al., 2021; Restrepo-Moreno et al., 2009; Zapata et al., 2021). For instance, shortening estimates of 40 ± 10 km in the Eastern Cordillera and Magdalena basin during the Miocene to recent between 6°N

Figure 9. (a) Present-day structural map of the Nazca and Caribbean slabs beneath northwestern South America as interpreted in this study. Farallon/Nazca (green), and Caribbean (black) contours represent the depths of the subducted slab resulting from our paleotectonic reconstruction and geophysical interpretation. As this map is derived from a quantitative paleotectonic reconstruction, the white contours (age of entrance in the trench) are consistent with the amount of plate subducted after the corresponding time. Dashed red lines indicate the slab tears interpreted from the tomographic model. Southern Caribbean plate boundary is in agreement with the slab breakoff proposed in this study. Black triangles show active magmatism. Big arrows indicate the current direction and velocity of plate motion relative to stable South America (Mora-Páez et al., 2019). (b) Three-dimensional view of the interpreted Nazca plate, highlighting the intercept between the tomographic section "g" in Figure 4, and the Nazca slab at its vertical-axis bending. Location of the cross-section in Figure 4. (c) Tomographic profiles shown in Figure 4.

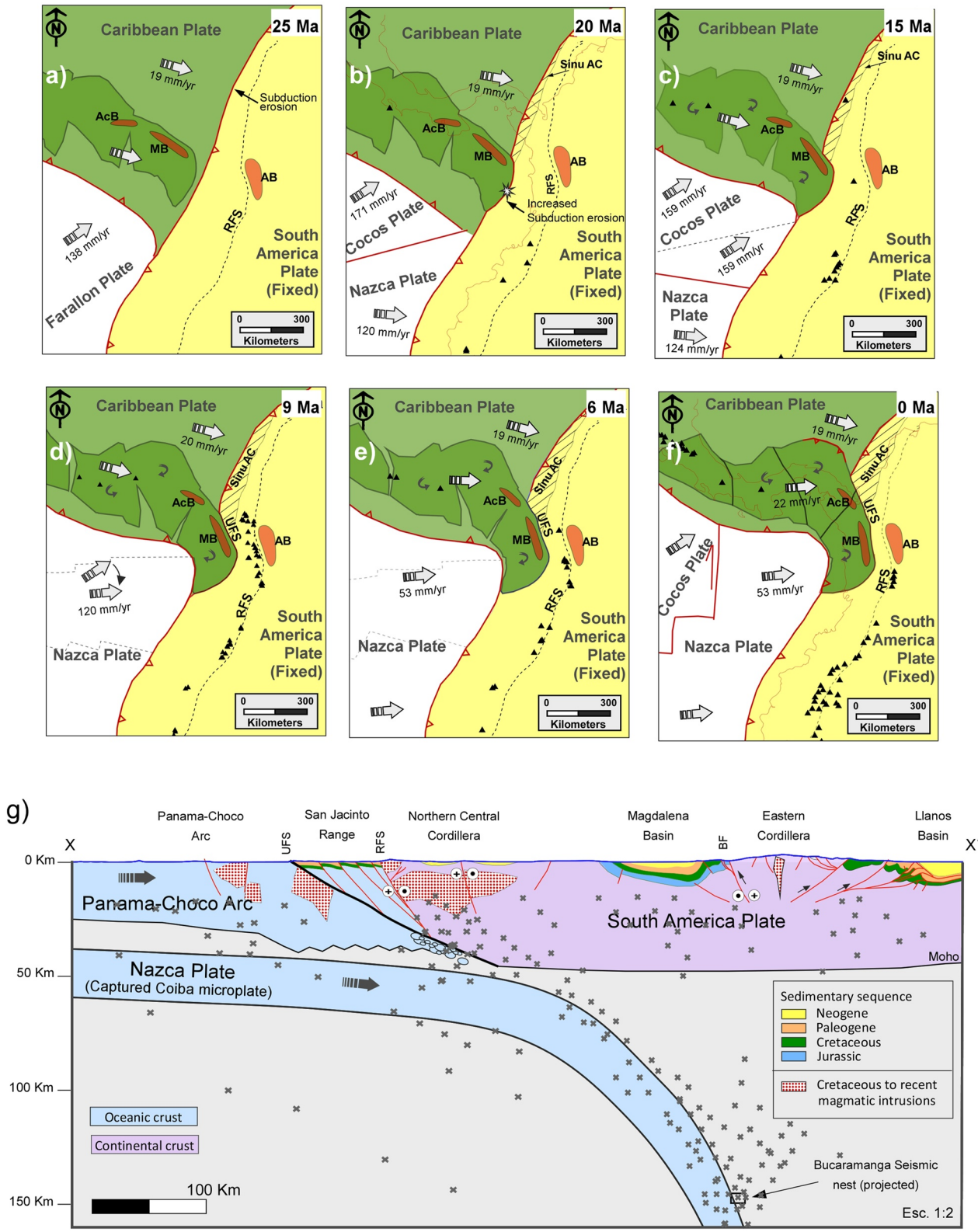

Figure 10.

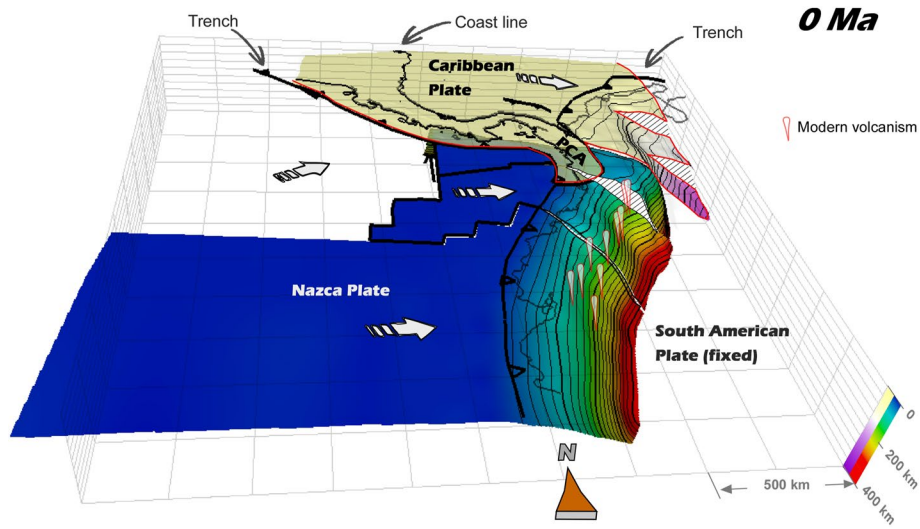

Figure 11. Three-dimensional view of the tectonic configuration proposed in this study for the Nazca and Caribbean plates at the junction between Central and South America (SA). The Nazca slab can be separated in two domains, a southern one with steep angle of subduction (>25°), and a northern one with flat-slab subduction that turns horizontally behind the PCA (Panama-Choco arc), following a similar geometry than the trench. On the other hand, the Caribbean slab consists of a shallow subducting slab that is tore apart to the east in three different segments. Note that the Caribbean slab is absent east of the PCA due to its breakoff during the middle Miocene. Nevertheless, the southern Caribbean edge overlaps the Nazca plate in its more northern segment. Directions of plate motion are relative to stable SA. Contour interval: 20 km.

and 8°N (Mora, Reyes-Harker, et al., 2013), and a maximum ∼10 km of shortening in the Central Cordillera during the same time span (range dominated by transpressive structures) give a total maximum shortening of ∼60 km, which is not compatible with 200 km of eastward advance of the margin. Moreover, León et al. (2018) recognize that the suture zone evolved as a negative topographic area, with the continuous accumulation of fine-grained hemipelagic sediments, precluding crustal thickening as a consequence of this contraction. The lack of known Miocene metamorphic rocks near the suture zone also suggests that this accretional process did not take place as a typical collisional event (Zheng et al., 2015) during the early Miocene. This is also confirmed by crustal thickness estimation from receiver functions by Poveda et al. (2015), showing no current crustal thickening in the suture zone. On the contrary, the Moho depth slightly decreases west of the Central Cordillera toward the suture.

Given that most of the original Paleogene forearc area is missing on the continental side (domain between the Uramita and the RFSs) (Figure 3b), we suggest that most parts of the forearc terrane (up to 200 km) were removed by subduction erosion during the emplacement of the PCA into the margin (Figure 11b). Despite subduction erosion is a major factor in removing material from active plate margins (e.g., Bruce et al., 2011; Clift & Vannucchi, 2004; Ranero and von Huene, 2000; Von Huene & Scholl, 1991), this process has not been proposed before to explain the accretion of the PCA to SA.

The tectonic erosion and fast trench advance margin in northwestern SA were likely a consequence of the hampered subduction of the highly buoyant lithosphere associated with the PCA, and the oceanic nature of the continental margin (mafic terrane accreted during the Late Cretaceous). Furthermore, the loss of at least 200 km of forearc material and trench advance since 20 Ma to the east of the PCA is similar to the average rate of 10 mm/yr of subduction erosion reported in the Peruvian margin associated with the subduction of the erosive Nazca

Figure 10. (a–f) Paleogeographic reconstruction of the Panama-Choco arc (PCA) convergence and accretion to the northwestern South Americ margin relative to South America (SA), showing the vertical axis rotation of blocks and orocline formation of the PCA (Montes et al., 2012), as well as the progressive loss of forearc crust in the continental side and consequent trench advance (triggered by severe subduction erosion). North of the collisional zone, it is shown that the slow convergence rate and increased sediment accumulation in the trench (Mora-Bohórquez, Oncken, et al., 2017) coincide with the formation of the Sinu accretionary prism. Black triangles show the location of paleo-active magmatism. Red polygons show the restored location of Cretaceous-Paleogene plutons. AB, Antioquia batholith and associated Paleogene stocks; AcB, Acandi batholith; MB, Mande batholith; RFS, Romeral fault system; Sinu Ac, Sinu accretionary prism; UFS, Uramita fault system. (g) Simplified cross-section showing the tectonic configuration. Location of the cross-section in Figure 3b. Black dots correspond to seismic events located within 8 km of the section. Crustal thickness for the South American plate taken from Poveda et al. (2015). Structural interpretation in the South American plate modified after Tesón et al. (2013) and Mora-Bohórquez, Ibánez-Mejia, et al. (2017).

ridge (Clift & Vannucchi, 2004). From numerical modeling, Keppie et al. (2009) find that regionally focused subduction erosion may occur in an unsteady fast mode that they show to have occurred along the Andean margin.

The lack of relevant exhumation pulses during the early Miocene could be due to the fact that erosive subduction systems are typically associated with subsidence in the forearc (e.g., Clift & Vannucchi, 2004; Kukowski & Oncken, 2006; Von Huene & Scholl, 1991), which supports the accumulation of an important Miocene sedimentary sequence of marine affinity, west of the RFS (Duque-Caro, 1990; J. Gómez et al., 2015; León et al., 2018), simultaneous with the initial accretion of the PCA.

Nonetheless, the forced subduction of a highly buoyant lithosphere could also lead to the rupture of the already subducted slabs (Figure 10b) (Zheng et al., 2015). Clear evidence that points to a slab breakoff beneath the NWSA margin is the development of Miocene arc-related magmatism in close proximity to the suture zone between the PCA and SA (Figures 3b, 8g, and 10d). These magmatic intrusions, ranging in age from 15 to 7 Ma (e.g.,Leal-Mejía et al., 2019), with heterogeneous compositions including tholeiitic, calc–alkaline, and shoshonitic signatures (Weber et al., 2020), have been regarded as originating from fluids from the Nazca slab (Wagner et al., 2017; Weber et al., 2020). Under the premise of an existing Caribbean slab (Figures S3f–S3h in Supporting Information S1), however, this magmatism would not be possible, as the fluids rising from the Nazca plate would be stopped by the overlaying Caribbean slab (which may have been subducting shallower than 50 km) (Figures S3f–S3h in Supporting Information S1). Therefore, the emplacement of these magmatic intrusions requires a breakoff in the Caribbean slab east of the PCA at about 15 Ma. This interpretation is corroborated by the regional trend of Miocene magmatism related to Pacific plates subduction (Figures 8f and 8g) and additionally, by the adakitic signature of these Miocene bodies (Weber et al., 2020). The latter could be related to the subduction of the active Sandra spreading center and to the complicated Nazca plate geometry behind the CSP triple junction. Moreover, the distribution of shallow seismicity (Figure 4a) indicates that the current deformation is not symmetrical on both sides of the suture, but it is significantly reduced east of the PCA side (east of the Uramita fault) (Figure 3a), coinciding with the area of no coupling by a Caribbean subducting slab.

We propose that the PCA was forced into the South American margin by means of a major subduction erosion of the forearc during the early Miocene (Figure 10d), with the consequent advance of the plate boundary. Subsequently, the hampered subduction of the highly buoyant arc resulted in the breakoff of the slab to the east of the PCA at about 15 Ma (Figure 8f), favoring initial margin subsidence and emplacement of Nazca-derived magmas in the upper plate. This interpretation, however, raises the question about the driving mechanism that supported the eastward motion of the PCA after initial collision. As suggested by published geodetic data, the Panama isthmus is currently moving at 22 mm/yr relative to stable SA, slightly faster than the current motion of the Caribbean plate (e.g., Trenkamp et al., 2002) (Figure 10f). Considering the late Miocene shallow subduction and the much faster Nazca plate, we speculate that the shallow Nazca kinematics boosted the motion of the overriding PCA microplate from below. Besides explaining the current kinematics of the PCA, this mechanism accounts for the continued approaching between the intra-oceanic and continental arcs (Mandé and Antioquia batholiths in Figures 10d–10f), which coincides with the increased deformation rate that initiated the main phase of the northern Andean orogeny. Additionally, the shallow and rapid subduction of the Nazca plate, which should have dragged the remnant detached segment of the Caribbean plate into the mantle, explains the lack of evidence of this segment in the tomography. This lack of evidence is also reinforced by experimental analyses that argue that detached slab segments are sunk into the mantle in a few million years (Duretz et al., 2011).

Even though the subduction mode of the Caribbean plate associated with the PCA accretion was highly erosive, it is interesting that the adjacent area to the north corresponds to a contemporaneous accretionary margin (Sinu accretionary prism) (Figure 10). Mora-Bohórquez, Ibánez-Mejia, et al. (2017) argue that the onset of the Sinu accretionary prism during the early Miocene following an earlier stage of subduction erosion was triggered by the initiation of massive influx of sediments from the Magdalena River to the trench. The PCA accretion could also play a role in this tectonic evolution. As suggested by Montes et al. (2015), the progressive closure of the Pacific-Atlantic seaway changed the oceanic currents during the Miocene, leading to the definitive separation of the Pacific and Atlantic oceans. The incremental restraining of oceanic currents could have favored the accumulation of the deltaic Magdalena sediments to the north of the PCA, favoring the formation of the Sinu accretionary prism in the Northern margin.

Finally, the kinematic reconstruction provides key arguments to propose that the southern Caribbean boundary beneath SA is located north of the accreted PCA. As previously suggested, following the initial erosive

subduction during the early Miocene, the physical impossibility of subducting thick and buoyant arc-related units (Mande Batholith) may have induced the slab breakup east of the PCA by the middle Miocene. An additional fact that restricts the Caribbean lithosphere to the north of 8°N, is that the PCA, as an island-arc is made up of a thick oceanic crust (e.g., J. Pindell et al., 2005) and underlain by sub-arc mantle lithosphere that is likely both very thin as well as weak due to its thermal state. If this thick arc is stacked against the South American plate, then there is no strong and thick mantle lithosphere to be subducted beneath SA east of the PCA. However, apart from the middle Miocene magmatism in northern Colombia (Figures 8f and 8g), there is no additional evidence to date for the onset of this condition. In Figures 8f–8h are shown the maximum southern edge of the Caribbean plate, estimated according to the magmatic development on SA, and the minimum southern edge derived from tracing the boundary of the PCA with the Caribbean lithosphere into the subduction zone using the Caribbean plate displacement since the collision of the PCA with SA.

5.3. Present-Day Tectonic Geometry

In order to validate the tectonic configuration resulting from the geometrical reconstruction of subduction, we developed a three-dimensional interpretation of the Nazca and Caribbean slabs based on seismicity data and the tomographic model of Sun et al. (2022) (Figure 4). The visualization—interpretation of these slabs within the tomographic model was made with the commercial software MOVE v. 2019 (https://www.petex.com) by using an orthogonal projection (Figures 9 and 11).

5.3.1. The Nazca Plate

The present-day Nazca slab can be separated into two domains separated by the Caldas tear at 5.5°N (Figure 9) (Vargas & Mann, 2013). The seismic distribution suggests that south of this position the Nazca plate subducts at a steep angle (>25°) (Figure 4b), which is further supported by the trend of the Andean magmatic arc (Andean Volcanic Zone), that is continuous south of this location (Pennington, 1981; Vargas & Mann, 2013; Wagner et al., 2017) (Figures 3 and 9a). Nonetheless, some authors have identified a velocity discontinuity at 3°N (N1 and N2 in Figures 4d–4f) (Sun et al., 2022; Vargas & Mann, 2013). However, the seismicity data do not show a significant change in geometry (Figure 4b). We regard this anomaly as a thermal perturbation possibly related to rising magmatic fluids, associated with the subduction of the extinct Malpelo rift. However, there is high uncertainty on the trace of this subducted rift (Figure 9a).

The interpretation of the Nazca plate, North of 5.5°N, is more difficult from the tomography, which has led to a number of different models in the past (Bernal-Olaya et al., 2015; Sun et al., 2022; Taboada et al., 2000; Vargas & Mann, 2013; Yarce et al., 2014). Taking this into account, we have based our interpretation mainly on the kinematic and geometrical modeling of the Farallon and Farallon-derived plates, which allow us to explain different observables in the geological record. A strength of this methodology is that the resulting present-day geometry of the Nazca plate is supported by velocity anomalies identified in the tomographic model (see description in Section 3.3; Figure 4). We consider that north of 5.5°N, the Nazca plate is comprised by a horizontally bending slab (or fragments of slabs), northeast of the CSP triple junction and (Figure 9), that seems to connect the subduction beneath the PCA and NWSA (see GIF image in Movie S1). It is important to consider that subduction along this tight corner may have resulted in different phases of slab rupture, which together with the subduction of the Sandra rift should be related to a young and warm slab. This condition could explain the weak nature of these velocity anomalies and the scarce seismicity east of the PCA (Figure 4b). Additionally, this interpretation is supported by the adakitic magmatic signature in eastern Panama (de Boer et al., 1988; Gutscher et al., 2000); the faster eastward motion of the Panama isthmus as compared to the Caribbean plate (as result of the Nazca slab pushing from below) (Figures 9a and 10g); the Miocene subduction-related magmatism north of 5.5°N (Weber et al., 2020), and the geometrical origin of the Farallon plate boundary as an Aleutian type margin (Cardona et al., 2018).

The Bucaramanga seismic nest (Figure 4b) has been related to either the Caribbean or the Nazca plate (e.g., Chiarabba et al., 2015; Prieto et al., 2012; Sun et al., 2022; Taboada et al., 2000; Vargas & Mann, 2013; Zarifi et al., 2007). According to our reconstruction, the Bucaramanga seismic nest is associated with the Nazca slab (Figure 10g). This interpretation is in line with the high eastward rate of subduction of the Nazca plate, and with other processes such as localized dehydration in the inflection point of the Nazca plate (Chiarabba et al., 2015; Siravo et al., 2019); the high strain rates at this bending geometry (Sun et al., 2022); thermal runaway processes

(Prieto et al., 2013), as well as complex mantle fluid dynamics that could be expected beneath this vertical-axis curved slab. Altogether, these factors could explain the relation between the Nazca plate and the Bucaramanga seismic nest. However, the lack of Nazca-related seismicity west of the vertical-axis bending and beneath Panama (Figure 4b) poses a challenge, which could be explained by the fact that today the Nazca slab has a negligible subduction motion in northward direction (Figure 9a).

5.3.2. The Caribbean Plate

In agreement with previous studies, our interpretation confirms that most of the Caribbean plate corresponds to a flat-slab (e.g., Cornthwaite et al., 2021; Mazuera et al., 2019; Sun et al., 2022) that decreases its dip toward the north (Figures 9a and 11). This shallow geometry is supported by a continuous northward trend of intermediate-depth seismicity (WBZ) at about 73°W (Figure 4b), which defines the position where the shallow subduction ends and the slab starts to sink into the mantle. In line with this observation, the kinematic reconstruction predicts that east of the WBZ, the current Caribbean slab may be fragmented as a result of cumulative instability in its leading edge due to the long subduction distance from the trench in northwestern Colombia (since the Eocene the slab has moved from west to east) (Figures 7b and 9a). This alternative interpretation is consistent with previous studies that suggest a no continuous Caribbean slab beneath northwestern Venezuela (Bezada et al., 2010; Sun et al., 2022; and references therein) and it is confirmed by the tomographic model (Figure 4h), which shows that east of 73°W the Caribbean slab is composed of three distinct step segments that are deeper to the south, likely separated by E-W tear faults.

Nonetheless, not all the intermediate-depth seismicity running from 5° to 10°N (Figure 4b) corresponds to the Caribbean plate. The southern edge of the Caribbean plate beneath SA is perhaps the most debated question that has not been resolved. Even though rocks of the Caribbean plate and PCA accreted to the continental margin during the Miocene are found between 4.5°N and 8°N (Duque-Caro, 1990), we conclude that it is not geodynamically possible to have remnants of the Caribbean slab subducting to the east of the accreted PCA (see Section 5 above). The simplest explanation is that there is no oceanic lithosphere beneath the stacked arc to feed the subduction system, nor is there a subduction trench (instead there is the Uramita suture zone, see Figure 3b). In addition to the deformation and magmatic record in the upper plate that support this hypothesis (see Section 5 above), the shallow and intermediate-depth seismicity, north of the Caldas tear, shows a subtle reduction between the Uramita fault zone and the WBZ at about 74°E (Figure 4a). This pattern of reduced seismicity is consistent with a missing Caribbean slab in that position. It is worth noting that the shallow subduction of the Nazca plate at this position, together with its fast Miocene to recent motion (120–53 mm/yr), may have dragged and sunk the detached Caribbean fragment into the mantle (Figure 10g) (Duretz et al., 2011), explaining its difficult identification in the tomography. Finally, it is important to remark that there is an area of close overlapping between the Nazca and Caribbean plates, as suggested in other studies (Figures 9 and 11) (e.g., Sun et al., 2022).

6. Conclusions

Our reconstruction indicates that the northeastward motion of the southern Caribbean edge caused a progressive change in the geometry of the Pacific trench, and in turn of the Farallon plate subduction (Figure S2 in Supporting Information S1). This change induced the flat-slab subduction of the Farallon plate throughout the late Eocene-late Oligocene, which inhibited the Farallon-related magmatism in the South American and PCA margins and facilitated the rupture of the Farallon plate. The subsequent plate kinematics during the early-middle Miocene induced a plate reorganization that included further plate fragmentation, change in convergence obliquity, steepening of the subducting slabs and renewing of magmatism. During the late Miocene, the Coiba and Malpelo microplates were attached to the Nazca plate, resulting in an abrupt change in convergence directions against eastern Panama and northern SA. This event correlates with the late Miocene onset of shallow subduction of the northernmost Nazca plate and the accelerated deformation in the Andes. Finally, during the late Pliocene, the flattened slab broke along the Caldas tear, triggering modern volcanism south of 5.5°N.

On the other side, the highly oblique convergence of the Caribbean plate during the Paleocene-Eocene allowed arc-related magmatism in northernmost SA. This configuration changed by the middle Eocene, when the Caribbean plate began to migrate in eastward direction relative to stable SA. This change triggered the breakoff of the slab and meant a significant lateral variation in obliquity along the margin. These factors prompted the slab-pull and flat-slab subduction from that moment onwards. By the late Oligocene-early Miocene, the approaching of

the buoyant PCA triggered the fragmentation and rotation of the PCA and a phase of rapid subduction erosion of the mafic forearc, accompanied by nearly 200 km of trench advance. By the middle Miocene, the Caribbean slab subduction could not continue, breaking this slab east of the PCA and initiating a phase of tectonic collision and a major phase of deformation in NWSA.

In summary, this contribution presents a paleotectonic reconstruction of the interacting Caribbean and Farallon/Nazca plates against NWSA that integrates the spatiotemporal distribution of magmatism and the first-order history of deformation in the northern Andes. The results of this reconstruction allowed us to constrain a new geometrical model of the subducting Caribbean and Nazca plates (Figure 11), which additionally explains key observables, such as seismicity and mantle velocity anomalies. Further works, including acquisitions of new seismological data and three-dimensional numerical and analog experiments, are required to test the proposed conceptual models and plate tectonic geometries.

Data Availability Statement

GPlates files from the paleotectonic reconstruction presented in this research are accessible as a Source Data file (González et al., 2023). The Data file additionally contains information including a compilation of the main tectonic events in the South American plate, and figures in three-dimensional view. However, the Zenodo repository has provided a new DOI for the data set (https://doi.org/10.5281/zenodo.8129751). The data set can be found here: https://zenodo.org/record/8129751.

Acknowledgments
This manuscript is part of the PhD research of R. Gonzalez at the Freie Universität Berlin and the GFZ Potsdam. R. González is especially grateful to Ecopetrol for funding this study. We acknowledge the GFZ Lithospheric Dynamics section for ongoing discussions, in particular Sabrina Metzger. We thank Robert Trumbull for his clarifications on subduction geodynamics. We are very grateful to German Bayona and an anonymous reviewer for their key comments and suggestions that contributed to improve the manuscript. Finally, R. González shows gratitude to Robert Ondrack and Alejandro Mora for their support in initiating this research. Open Access funding enabled and organized by Projekt DEAL.

References

Adamek, S., Frohlich, C., & Pennington, W. D. (1988). Seismicity of the Caribbean-Nazca boundary: Constraints on microplate tectonics of the Panama region. *Journal of Geophysical Research*, *93*(B3), 2053–2075. https://doi.org/10.1029/jb093ib03p02053

Amante, C., & Eakins, B. W. (2009). *ETOPO1 arc-minute global relief model: Procedures, data sources and analysis*. NOAA/National Oceanic and Atmospheric Administration. National Environmental Satellite, Data, and Information Service.

Andrić-Tomašević, N., Koptev, A., Maiti, G., Gerya, T., & Ehlers, T. A. (2023). Slab tearing in non-collisional settings: Insights from thermo-mechanical modelling of oblique subduction. *Earth and Planetary Science Letters*, *610*, 118097. https://doi.org/10.1016/j.epsl.2023.118097

Barat, F., Mercier de Lépinay, B., Sosson, M., Müller, C., Baumgartner, P. O., & Baumgartner-Mora, C. (2014). Transition from the Farallon Plate subduction to the collision between South and central America. *Geological evolution of the Panama Isthmus: Tectonophysics*, *622*, 145–167. https://doi.org/10.1016/j.tecto.2014.03.008

Barbosa-Espitia, Á. A., Kamenov, G. D., Foster, D. A., Restrepo-Moreno, S. A., & Pardo-Trujillo, A. (2019). Contemporaneous Paleogene arc-magmatism within continental and accreted oceanic arc complexes in the northwestern Andes and Panama. *Lithos*, *348–349*, 105185. https://doi.org/10.1016/j.lithos.2019.105185

Barckhausen, U., Ranero, C. R., von Huene, R., Cande, S. C., & Roeser, H. A. (2001). Revised tectonic boundaries in the Cocos Plate off Costa Rica: Implications for the segmentation of the convergent margin and for plate tectonic models. *Journal of Geophysical Research*, *106*(B9), 19207–19220. https://doi.org/10.1029/2001jb000238

Bayona, G., Baquero, M., Ramírez, C., Tabares, M., Salazar, A. M., Nova, G., et al. (2020). Unravelling the widening of the earliest Andean northern orogen: Maastrichtian to early Eocene intra-basinal deformation in the northern Eastern Cordillera of Colombia. *Basin Research*, *33*(1), 809–845. https://doi.org/10.1111/bre.12496

Bayona, G., Cardona, A., Jaramillo, C., Mora, A., Montes, C., Caballero, V., et al. (2013). *Onset of fault reactivation in the Eastern Cordillera of Colombia and proximal Llanos Basin; response to Caribbean–South American convergence in early Palaeogene time* (Vol. 377, p. 285). Geological Society, London, Special Publications.

Bayona, G., Cardona, A., Jaramillo, C., Mora, A., Montes, C., Valencia, V., et al. (2012). Early Paleogene magmatism in the northern Andes: Insights on the effects of Oceanic Plateau–continent convergence. *Earth and Planetary Science Letters*, *331–332*, 97–111. https://doi.org/10.1016/j.epsl.2012.03.015

Bernal-Olaya, R., Mann, P., & Vargas, C. (2015). Earthquake, tomographic, seismic reflection, and gravity evidence for a shallowly dipping subduction zone beneath the Caribbean margin of northwestern Colombia. In *AAPG Memoir* (Vol. 108, p. 22).

Bernet, M., Urueña, C., Amaya, S., & Peña, M. L. (2016). New thermo and geochronological constraints on the Pliocene-Pleistocene eruption history of the Paipa-Iza volcanic complex, Eastern Cordillera, Colombia. *Journal of Volcanology and Geothermal Research*, *327*, 299–309. https://doi.org/10.1016/j.jvolgeores.2016.08.013

Bezada, M. J., Levander, A., & Schmandt, B. (2010). Subduction in the southern Caribbean: Images from finite-frequency P wave tomography. *Journal of Geophysical Research*, *115*(B12), B12333. https://doi.org/10.1029/2010jb007682

Blanquat, M. D. S., Tikoff, B., Teyssier, C., & Vigneresse, J. L. (1998). Transpressional kinematics and magmatic arcs. *Geological Society, London, Special Publications*, *135*(1), 327–340. https://doi.org/10.1144/gsl.sp.1998.135.01.21

Boschman, L. M., van Hinsbergen, D. J. J., Torsvik, T. H., Spakman, W., & Pindell, J. L. (2014). Kinematic reconstruction of the Caribbean region since the early Jurassic. *Earth-Science Reviews*, *138*, 102–136. https://doi.org/10.1016/j.earscirev.2014.08.007

Bourgois, J., Lagabrielle, Y., Martin, H., Dyment, J., Frutos, J., & Cisternas, M. E. (2016). A review on forearc ophiolite obduction, Adakite-like generation, and slab window development at the Chile triple junction area: Uniformitarian framework for spreading-ridge subduction. *Pure and Applied Geophysics*, *173*(10–11), 3217–3246. https://doi.org/10.1007/s00024-016-1317-9

Boyden, J. A., Müller, R. D., Gurnis, M., Torsvik, T. H., Clark, J. A., Turner, M., et al. (2011). Next-generation plate-tectonic reconstructions using GPlates. In C. Baru & G. R. Keller (Eds.), *Geoinformatics: Cyberinfrastructure for the solid earth sciences* (pp. 95–114). Cambridge University Press.

Bruce, J., Shyu, H., Wu, Y.-M., Chang, C.-H., & Huang, H.-H. (2011). Tectonic erosion and the removal of forearc lithosphere during arc-continent collision: Evidence from recent earthquake sequences and tomography results in eastern Taiwan. *Journal of Asian Earth Sciences*, *42*(3), 415–422. https://doi.org/10.1016/j.jseaes.2011.05.015

Burke, K. (1988). Tectonic evolution of the Caribbean. *Annual Review of Earth and Planetary Sciences*, *16*(1), 201–230. https://doi.org/10.1146/annurev.ea.16.050188.001221

Caballero, V., Parra, M., Mora, A., López, C., Rojas, L. E., & Quintero, I. (2013). Factors controlling selective abandonment and reactivation in thick-skin orogens: A case study in the Magdalena Valley, Colombia. *Geological Society, London, Special Publications*, *377*(1), 343–367. https://doi.org/10.1144/sp377.4

Cardona, A., León, S., Jaramillo, J. S., Montes, C., Valencia, V., Vanegas, J., et al. (2018). The Paleogene arcs of the northern Andes of Colombia and Panama: Insights on plate kinematic implications from new and existing geochemical, geochronological and isotopic data. *Tectonophysics*, *749*, 88–103. https://doi.org/10.1016/j.tecto.2018.10.032

Cardona, A., Valencia, V., Weber, M., Duque, J., Montes, C., Ojeda, G., et al. (2011). Transient Cenozoic tectonic stages in the southern margin of the Caribbean plate: U-Th/He thermochronological constraints from Eocene plutonic rocks in the Santa Marta massif and Serrania de Jarara, northern Colombia. *Geológica Acta*, *9*, 445.

Cardona, A., Weber, M., Valencia, V., Bustamante, C., Montes, C., Cordani, U., & Muñoz, C. M. (2014). Geochronology and geochemistry of the Parashi granitoid, NE Colombia: Tectonic implication of short-lived Early Eocene plutonism along the SE Caribbean margin. *Journal of South American Earth Sciences*, *50*, 75–92. https://doi.org/10.1016/j.jsames.2013.12.006

Carrillo, E., Mora, A., Ketcham, R. A., Amorocho, R., Parra, M., Costantino, D., et al. (2016). Movement vectors and deformation mechanisms in kinematic restorations: A case study from the Colombian eastern cordillera. *Interpretation*, *4*(1), T31–T48. https://doi.org/10.1190/int-2015-0049.1

Cediel, F., Shaw, R. P., & Cáceres, C. (2003). Tectonic Assembly of the northern Andean block. In C. Bartolini, R. T. Buffler, & J. F. Blickwede (Eds.), *The Circum-Gulf of Mexico and the Caribbean: Hydrocarbon habitats, basin formation and plate tectonics*. American Association of Petroleum Geologists.

Chiarabba, C., De Gori, P., Faccenna, C., Speranza, F., Seccia, D., Dionicio, V., & Prieto, G. A. (2015). Subduction system and flat slab beneath the Eastern Cordillera of Colombia. *Geochemistry, Geophysics, Geosystems*, *17*(1), 16–27. https://doi.org/10.1002/2015gc006048

Clift, P., & Vannucchi, P. (2004). Controls on tectonic accretion versus erosion in subduction zones: Implications for the origin and recycling of the continental crust. *Reviews of Geophysics*, *42*(2), RG2001. https://doi.org/10.1029/2003rg000127

Coira, B., Davidson, J., Mpodozis, C., & Ramos, V. (1982). Tectonic and magmatic evolution of the Andes of northern Argentina and Chile. *Earth-Science Reviews*, *18*(3–4), 302–332. https://doi.org/10.1016/0012-8252(82)90042-3

Cornthwaite, J., Bezada, M. J., Miao, W., Schmitz, M., Prieto, G. A., Dionicio, V., et al. (2021). Caribbean slab segmentation beneath northwest South America revealed by 3-D finite frequency teleseismic P-wave tomography. *Geochemistry, Geophysics, Geosystems*, *22*(4), e2020GC009431. https://doi.org/10.1029/2020gc009431

Cortés, M., & Angelier, J. (2005). Current states of stress in the northern Andes as indicated by focal mechanisms of earthquakes. *Tectonophysics*, *403*(1–4), 29–58. https://doi.org/10.1016/j.tecto.2005.03.020

de Boer, J. Z., Defant, M. J., Stewart, R. H., Restrepo, J. F., Clark, L. F., & Ramirez, A. H. (1988). Quaternary calc-alkaline volcanism in western Panama: Regional variation and implication for the plate tectonic framework. *Journal of South American Earth Sciences*, *1*(3), 275–293. https://doi.org/10.1016/0895-9811(88)90006-5

de la Parra, F., Mora, A., Rueda, M., & Quintero, I. (2015). Temporal and spatial distribution of tectonic events as deduced from reworked palynomorphs in the eastern northern Andes. *AAPG Bulletin*, *99*(08), 1455–1472. https://doi.org/10.1306/02241511153

Di Marco, G., Baumgartner, P. O., & Channell, J. E. (1995). Late Cretaceous—Early Tertiary paleomagnetic data and a revised tectonostratigraphic subdivision of Costa Rica and western Panama. In *Geologic and tectonic development of the Caribbean plate boundary in southern Central America, v. Special paper 295*. Geological Society of America.

Duque-Caro, H. (1990). The Choco block in the northwestern corner of South America: Structural, tectonostratigraphic, and paleogeographic implications. *Journal of South American Earth Sciences*, *3*(1), 71–84. https://doi.org/10.1016/0895-9811(90)90019-w

Duretz, T., Gerya, T. V., & May, D. A. (2011). Numerical modelling of spontaneous slab breakoff and subsequent topographic response. *Tectonophysics*, *502*(1–2), 244–256. https://doi.org/10.1016/j.tecto.2010.05.024

Escalona, A., & Mann, P. (2011). Tectonics, basin subsidence mechanisms, and paleogeography of the Caribbean-South American plate boundary zone. *Marine and Petroleum Geology*, *28*(1), 8–39. https://doi.org/10.1016/j.marpetgeo.2010.01.016

Etayo-Serna, F. (1983). The Georgian heteromorph ammonite genera Kutatissites and Pseudoaustraliceras in northwest South America. *Geologia Norandina*, *7*, 3–13.

Faccenna, C., Holt, A. F., Becker, T. W., Lallemand, S., & Royden, L. H. (2018). Dynamics of the Ryukyu/Izu-Bonin-Marianas double subduction system. *Tectonophysics*, *746*, 229–238. https://doi.org/10.1016/j.tecto.2017.08.011

Farris, D. W., Jaramillo, C., Bayona, G., Restrepo-Moreno, S. A., Montes, C., Cardona, A., et al. (2011). Fracturing of the Panamanian isthmus during initial collision with South America. *Geology*, *39*(11), 1007–1010. https://doi.org/10.1130/g32237.1

Gansser, A. (1973). Facts and theories on the Andes: Twenty-sixth William Smith lecture. *Journal of the Geological Society*, *129*(2), 93–131. https://doi.org/10.1144/gsjgs.129.2.0093

Geldmacher, J., Höfig, T. W., Hauff, F., Hoernle, K., Garbe-Schönberg, D., & Wilson, D. S. (2013). Influence of the Galápagos hotspot on the East Pacific rise during Miocene superfast spreading. *Geology*, *41*(2), 183–186. https://doi.org/10.1130/g33533.1

Gómez, E. A., Jordan, T. E., Allmendinger, R. W., Hegarty, K., Kelley, S., & Heizler, M. (2003). Controls on architecture of the Late Cretaceous to Cenozoic southern middle Magdalena Valley basin, Colombia. *GSA Bulletin*, *115*, 131–147. https://doi.org/10.1130/0016-7606(2003)115<0131:coaotl>2.0.co;2

Gómez, J., Montes, N. E., Nivia, Á., & Diederix, H. (2015). Geological map of Colombia 2015. Scale 1:1 000 000. Servicio Geológico Colombiano, 2 sheets. Bogotá. https://doi.org/10.32685/10.143.2015.936

González, R., Oncken, O., Faccenna, C., & Breton, E. (2023). Kinematics and convergent tectonics of the Northwestern South American plate during the Cenozoic [Dataset]. Zenodo. https://doi.org/10.5281/zenodo.7411340

Govers, R., & Wortel, M. J. R. (2005). Lithosphere tearing at STEP faults: Response to edges of subduction zones. *Earth and Planetary Science Letters*, *236*(1–2), 505–523. https://doi.org/10.1016/j.epsl.2005.03.022

Grajales, J. A., Nieto-Samaniego, Á. F., Barrero-Lozano, D., Osorio, J. A., & Cuellar, M. A. (2020). Emplazamiento del magmatismo Paleoceno-Eoceno bajo un régimen transtensional y su evolución a un equilibrio dinámico en el borde Occidental de Colombia. *Revista Mexicana de Ciencias Geológicas*, *37*(3), 250–268. https://doi.org/10.22201/cgeo.20072902e.2020.3.1570

Guivel, C., Lagabrielle, Y., Bourgois, J., Martin, H., Arnaud, N., Fourcade, S., et al. (2003). Very shallow melting of oceanic crust during spreading ridge subduction: Origin of near-trench Quaternary volcanism at the Chile Triple Junction. *Journal of Geophysical Research*, *108*(B7), ECV7.1–ECV7.19. https://doi.org/10.1029/2002jb002119

Gurnis, M., Turner, M., Zahirovic, S., DiCaprio, L., Spasojevic, S., Müller, R. D., et al. (2012). Plate tectonic reconstructions with continuously closing plates. *Computers & Geosciences*, *38*(1), 35–42. https://doi.org/10.1016/j.cageo.2011.04.014

Gurnis, M., Yang, T., Cannon, J., Turner, M., Williams, S., Flament, N., & Müller, R. D. (2018). Global tectonic reconstructions with continuously deforming and evolving rigid plates. *Computers & Geosciences*, *116*, 32–41. https://doi.org/10.1016/j.cageo.2018.04.007

Gutscher, M.-A., Maury, R., Eissen, J.-P., & Bourdon, E. (2000). Can slab melting be caused by flat subduction? *Geology*, *28*(6), 535–538. https://doi.org/10.1130/0091-7613(2000)028<0535:csmbcb>2.3.co;2

Handschumacher, D. W. (1976). Post-Eocene plate tectonics of the Eastern Pacific: The Geophysics of the Pacific Ocean basin and its margin (pp. 177–202).

Hardy, N. C. (1991). Tectonic evolution of the easternmost Panama basin: Some new data and inferences. *Journal of South American Earth Sciences*, *4*(3), 261–269. https://doi.org/10.1016/0895-9811(91)90035-j

Horton, B. K., Anderson, V. J., Caballero, V., Saylor, J. E., Nie, J., Parra, M., & Mora, A. (2015). Application of detrital zircon U-Pb geochronology to surface and subsurface correlations of provenance, paleodrainage, and tectonics of the Middle Magdalena Valley Basin of Colombia. *Geosphere*, *11*(6), 1790–1811. https://doi.org/10.1130/ges01251.1

Jaramillo, J. S., Cardona, A., León, S., Valencia, V., & Vinasco, C. (2017). Geochemistry and geochronology from Cretaceous magmatic and sedimentary rocks at 6°35′N, western flank of the Central cordillera (Colombian Andes): Magmatic record of arc growth and collision. *Journal of South American Earth Sciences*, *76*, 460–481. https://doi.org/10.1016/j.jsames.2017.04.012

Johnston, S. T., & Thorkelson, D. J. (1997). Cocos-Nazca slab window beneath Central America. *Earth and Planetary Science Letters*, *146*(3–4), 465–474. https://doi.org/10.1016/s0012-821x(96)00242-7

Kellogg, J. N., Camelio, G. B. F., & Mora-Páez, H. (2019). Chapter 4—Cenozoic tectonic evolution of the North Andes with constraints from volcanic ages, seismic reflection, and satellite geodesy. In B. K. Horton & A. Folguera (Eds.), *Andean tectonics* (pp. 69–102). Elsevier.

Keppie, D. F., Currie, C. A., & Warren, C. (2009). Subduction erosion modes: Comparing finite element numerical models with the geological record. *Earth and Planetary Science Letters*, *287*(1–2), 241–254. https://doi.org/10.1016/j.epsl.2009.08.009

Kerr, A. C., & Tarney, J. (2005). Tectonic evolution of the Caribbean and northwestern South America: The case for accretion of two Late Cretaceous oceanic plateaus. *Geology*, *33*(4), 269–272. https://doi.org/10.1130/g21109.1

Kerr, A. C., Tarney, J., Marriner, G. F., Nivia, A., & Saunders, A. D. (1997). The Caribbean-Colombian Cretaceous igneous province: The internal anatomy of an oceanic plateau. *Geophysical monograph-American Geophysical Union*, *100*, 123–144.

Kroehler, M. E., Mann, P., Escalona, A., & Christeson, G. (2011). Late Cretaceous-Miocene diachronous onset of back thrusting along the South Caribbean deformed belt and its importance for understanding processes of arc collision and crustal growth. *Tectonics*, *30*(6), TC6003. https://doi.org/10.1029/2011TC002918

Kukowski, N., & Oncken, O. (2006). *Subduction erosion—The "normal" mode of fore-arc material transfer along the Chilean margin?, the Andes* (pp. 217–236). Springer.

Lara, M., Cardona, A., Monsalve, G., Yarce, J., Montes, C., Valencia, V., et al. (2013). Middle Miocene near trench volcanism in northern Colombia: A record of slab tearing due to the simultaneous subduction of the Caribbean plate under South and central America? *Journal of South American Earth Sciences*, *45*, 24–41. https://doi.org/10.1016/j.jsames.2012.12.006

Leal-Mejía, H., Shaw, R. P., & Melgarejo i Draper, J. C. (2019). *Spatial-temporal migration of granitoid magmatism and the Phanerozoic tectono-magmatic evolution of the Colombian Andes, Geology and tectonics of Northwestern South America* (pp. 253–410). Springer.

León, S., Cardona, A., Parra, M., Sobel, E. R., Jaramillo, J. S., Glodny, J., et al. (2018). Transition from collisional to subduction-related regimes: An example from Neogene Panama-Nazca-South America interactions. *Tectonics*, *37*(1), 119–139. https://doi.org/10.1002/2017tc004785

Lissinna, B. (2005). A profile through the central American landbridge in western Panama: 115 Ma interplay between the Galápagos hotspot and the central American subduction zone.

Lonsdale, P. (2005). Creation of the Cocos and Nazca plates by fission of the Farallon plate. *Tectonophysics*, *404*(3–4), 237–264. https://doi.org/10.1016/j.tecto.2005.05.011

MacMillan, I., Gans, P. B., & Alvarado, G. (2004). Middle Miocene to present plate tectonic history of the southern Central American Volcanic Arc. *Tectonophysics*, *392*(1–4), 325–348. https://doi.org/10.1016/j.tecto.2004.04.014

Mann, P. (1999). Chapter 1 Caribbean sedimentary basins: Classification and tectonic setting from Jurassic to present. In P. Mann (Ed.), *Sedimentary basins of the world* (Vol. 4, pp. 3–31). Elsevier.

Mann, P., & Kolarsky, R. A. (1995). East Panama deformed belt: Structure, age, and neotectonic significance: Special papers-Geological Society of America (p. 111).

Marín-Cerón, M. I., Leal-Mejía, H., Bernet, M., & Mesa-García, J. (2019). *Late Cenozoic to modern-day volcanism in the Northern Andes: A geochronological, petrographical, and geochemical review, Geology and tectonics of Northwestern South America* (pp. 603–648). Springer.

Martinez, J., Patiño, M., Mora, A., Arias Martínez, J. P., & Tesón, E. (2022). Chapter 13—Structural styles and evolution of the Colombian Eastern foothills Piedemonte triangle zone. In G. Zamora & A. Mora (Eds.), *Andean structural styles* (pp. 181–193). Elsevier.

Matthews, K. J., Maloney, K. T., Zahirovic, S., Williams, S. E., Seton, M., & Müller, R. D. (2016). Global plate boundary evolution and kinematics since the late Paleozoic. *Global and Planetary Change*, *146*, 226–250. https://doi.org/10.1016/j.gloplacha.2016.10.002

Mazuera, F., Schmitz, M., Escalona, A., Zelt, C., & Levander, A. (2019). Lithospheric structure of northwestern Venezuela from wide-angle seismic data: Implications for the understanding of continental margin evolution. *Journal of Geophysical Research: Solid Earth*, *124*(12), 13124–13149. https://doi.org/10.1029/2019jb017892

McGirr, R., Seton, M., & Williams, S. (2020). Kinematic and geodynamic evolution of the isthmus of Panama region: Implications for central American seaway closure. *GSA Bulletin*, *133*(3–4), 867–884. https://doi.org/10.1130/b35595.1

Meschede, M., & Frisch, W. (1998). A plate-tectonic model for the Mesozoic and Early Cenozoic history of the Caribbean plate. *Tectonophysics*, *296*(3–4), 269–291. https://doi.org/10.1016/s0040-1951(98)00157-7

Montes, C., Bayona, G., Cardona, A., Buchs, D. M., Silva, C. A., Morón, S., et al. (2012). Arc-continent collision and orocline formation: Closing of the Central American seaway. *Journal of Geophysical Research*, *117*(B4), 4105. https://doi.org/10.1029/2011jb008959

Montes, C., Cardona, A., Jaramillo, C., Pardo, A., Silva, J. C., Valencia, V., et al. (2015). Middle Miocene closure of the central American seaway. *Science*, *348*(6231), 226–229. https://doi.org/10.1126/science.aaa2815

Montes, C., Rodriguez-Corcho, A. F., Bayona, G., Hoyos, N., Zapata, S., & Cardona, A. (2019). Continental margin response to multiple arc-continent collisions: The northern Andes-Caribbean margin. *Earth-Science Reviews*, *198*, 102903. https://doi.org/10.1016/j.earscirev.2019.102903

Moore, G. F., Sender, K. L., & Mann, P. (1995). Fracture zone collision along the South Panama margin: Special papers-Geological Society of America (p. 201).

Mora, A., Blanco, V., Naranjo, J., Sanchez, N., Ketcham, R. A., Rubiano, J., et al. (2013). On the lag time between internal strain and basement involved thrust induced exhumation: The case of the Colombian Eastern Cordillera. *Journal of Structural Geology*, *52*, 96–118. https://doi.org/10.1016/j.jsg.2013.04.001

Mora, A., Horton, B. K., Mesa, A. S., Rubiano, J., Ketcham, R. A., Parra, M., et al. (2010). Migration of Cenozoic deformation in the Eastern Cordillera of Colombia interpreted from fission track results and structural relationships: Implications for petroleum systems. *AAPG Bulletin*, *94*(10), 1543–1580. https://doi.org/10.1306/01051009111

Mora, A., Parra, M., Forero, G. R., Blanco, V., Moreno, N., Caballero, V., et al. (2015). What drives orogenic asymmetry in the Northern Andes?: A case study from the apex of the Northern Andean Orocline.

Mora, A., Parra, M., Strecker, M. R., Kammer, A., Dimaté, C., & Rodríguez, F. (2006). Cenozoic contractional reactivation of Mesozoic extensional structures in the Eastern Cordillera of Colombia. *Tectonics*, *25*(2), 19. https://doi.org/10.1029/2005tc001854

Mora, A., Reyes-Harker, A., Rodriguez, G., Tesón, E., Ramirez-Arias, J. C., Parra, M., et al. (2013). Inversion tectonics under increasing rates of shortening and sedimentation: Cenozoic example from the Eastern Cordillera of Colombia. *Geological Society, London, Special Publications*, *377*(1), 411–442. https://doi.org/10.1144/sp377.6

Mora, A., Tesón, E., Martínez, J., Parra, M., Lasso, A., Horton, B. K., et al. (2020). The eastern foothills of Colombia. In *The geology of Colombia* (Vol. 3, pp. 123–142).

Mora, A., Villagómez, D., Parra, M., Caballero, V. M., Spikings, R., Horton, B. K., et al. (2020). Late Cretaceous to Cenozoic uplift of the northern Andes: Paleogeographic implications. In *The geology of Colombia* (Vol. 3, pp. 89–121).

Mora-Bohórquez, J. A., Ibánez-Mejia, M., Oncken, O., de Freitas, M., Vélez, V., Mesa, A., & Serna, L. (2017). Structure and age of the Lower Magdalena Valley basin basement, northern Colombia: New reflection-seismic and U-Pb-Hf insights into the termination of the central andes against the Caribbean basin. *Journal of South American Earth Sciences*, *74*, 1–26. https://doi.org/10.1016/j.jsames.2017.01.001

Mora-Bohórquez, J. A., Oncken, O., Le Breton, E., Ibánez-Mejia, M., Faccenna, C., Veloza, G., et al. (2017). Linking Late Cretaceous to Eocene tectonostratigraphy of the San Jacinto fold belt of NW Colombia with Caribbean plateau collision and flat subduction. *Tectonics*, *36*(11), 2599–2629. https://doi.org/10.1002/2017tc004612

Mora-Bohórquez, J. A., Oncken, O., Le Breton, E., Mora, A., Veloza, G., Vélez, V., & de Freitas, M. (2018). Controls on forearc basin formation and evolution: Insights from Oligocene to Recent tectono-stratigraphy of the Lower Magdalena Valley basin of northwest Colombia. *Marine and Petroleum Geology*, *97*, 288–310. https://doi.org/10.1016/j.marpetgeo.2018.06.032

Mora-Páez, H., Kellogg, J. N., Freymueller, J. T., Mencin, D., Fernandes, R. M. S., Diederix, H., et al. (2019). Crustal deformation in the northern Andes—A new GPS velocity field. *Journal of South American Earth Sciences*, *89*, 76–91. https://doi.org/10.1016/j.jsames.2018.11.002

Morell, K. D. (2015). Late Miocene to recent plate tectonic history of the southern Central America convergent margin. *Geochemistry, Geophysics, Geosystems*, *16*(10), 3362–3382. https://doi.org/10.1002/2015gc005971

Moreno, N., Silva, A., Mora, A., Tesón, E., Quintero, I., Rojas, L. E., et al. (2013). Interaction between thin-and thick-skinned tectonics in the foothill areas of an inverted graben. The Middle Magdalena Foothill belt. *Geological Society, London, Special Publications*, *377*(1), 221–255. https://doi.org/10.1144/sp377.18

Müller, R. D., Cannon, J., Qin, X., Watson, R. J., Gurnis, M., Williams, S., et al. (2018). GPlates: Building a virtual Earth through deep time. *Geochemistry, Geophysics, Geosystems*, *19*(7), 2243–2261. https://doi.org/10.1029/2018gc007584

Müller, R. D., Zahirovic, S., Williams, S. E., Cannon, J., Seton, M., Bower, D. J., et al. (2019). A global plate model including lithospheric deformation along major rifts and orogens since the Triassic. *Tectonics*, *38*(6), 1884–1907. https://doi.org/10.1029/2018tc005462

Oncken, O., Hindle, D., Kley, J., Elger, K., Victor, P., & Schemmann, K. (2006). *Deformation of the central Andean upper plate system—Facts, fiction, and constraints for plateau models, the Andes* (pp. 3–27). Springer.

Pardo, N., Cepeda, H., & Jaramillo, J. M. (2005). The Paipa volcano, eastern cordillera of Colombia, South America: Volcanic stratigraphy. *Earth Sciences Research Journal*, *9*, 3–18.

Pardo-Casas, F., & Molnar, P. (1987). Relative motion of the Nazca (Farallon) and South American plates since Late Cretaceous time. *Tectonics*, *6*(3), 233–248. https://doi.org/10.1029/tc006i003p00233

Pardo-Trujillo, A., Echeverri, S., Borrero, C., Arenas, A., Vallejo, F., Trejos, R., et al. (2020). Cenozoic geologic evolution of the southern Tumaco forearc basin (SW Colombian Pacific). In *The geology of Colombia* (Vol. 3, pp. 215–247).

Parra, M., Mora, A., Sobel, E. R., Strecker, M. R., & González, R. (2009). Episodic orogenic front migration in the northern Andes: Constraints from low-temperature thermochronology in the Eastern Cordillera, Colombia. *Tectonics*, *28*(4), TC4004. https://doi.org/10.1029/2008tc002423

Pennington, W. D. (1981). Subduction of the eastern Panama basin and seismotectonics of Northwestern South America. *Journal of Geophysical Research*, *86*(B11), 10753–10770. https://doi.org/10.1029/jb086ib11p10753

Pérez-Consuegra, N., Ott, R. F., Hoke, G. D., Galve, J. P., Pérez-Peña, V., & Mora, A. (2021). Neogene variations in slab geometry drive topographic change and drainage reorganization in the Northern Andes of Colombia. *Global and Planetary Change*, *206*, 103641. https://doi.org/10.1016/j.gloplacha.2021.103641

Pindell, J., Kennan, L., Maresch, W. V., Stanek, K., Draper, G., & Higgs, R. (2005). Plate-kinematics and crustal dynamics of circum-Caribbean arc-continent interactions: Tectonic controls on basin development in Proto-Caribbean margins. In *Special papers-Geological Society of America* (Vol. 394, p. 7).

Pindell, J. L., & Barrett, S. F. (1990). Caribbean plate tectonic history: The Caribbean region, volume H of the Geology of North America (pp. 405–432).

Pindell, J. L., & Kennan, L. (2009). *Tectonic evolution of the Gulf of Mexico, Caribbean and northern South America in the mantle reference frame: An update* (Vol. 328, pp. 1–55). Geological Society, London, Special Publications.

Poveda, E., Monsalve, G., & Vargas, C. A. (2015). Receiver functions and crustal structure of the northwestern Andean region, Colombia. *Journal of Geophysical Research: Solid Earth*, *120*(4), 2408–2425. https://doi.org/10.1002/2014jb011304

Prieto, G. A., Beroza, G. C., Barrett, S. A., López, G. A., & Florez, M. (2012). Earthquake nests as natural laboratories for the study of intermediate-depth earthquake mechanics. *Tectonophysics*, *570–571*, 42–56. https://doi.org/10.1016/j.tecto.2012.07.019

Prieto, G. A., Florez, M., Barrett, S. A., Beroza, G. C., Pedraza, P., Blanco, J. F., & Poveda, E. (2013). Seismic evidence for thermal runaway during intermediate-depth earthquake rupture. *Geophysical Research Letters*, *40*(23), 6064–6068. https://doi.org/10.1002/2013gl058109

Ramos, V. A. (2010). The tectonic regime along the Andes: Present-day and Mesozoic regimes. *Geological Journal*, *45*(1), 2–25. https://doi.org/10.1002/gj.1193

Ramos, V. A., Cristallini, E. O., & Pérez, D. J. (2002). The Pampean flat-slab of the central Andes. *Journal of South American Earth Sciences*, *15*(1), 59–78. https://doi.org/10.1016/s0895-9811(02)00006-8

Ranero, C. R., & von Huene, R. (2000). Subduction erosion along the Middle America convergent margin. *Nature*, *404*(6779), 748–752. https://doi.org/10.1038/35008046

Restrepo, J. J., & Toussaint, J. F. (1988). *Terranes and continental accretion in the Colombian Andes* (Vol. 11, pp. 189–193). International Union of Geological Sciences.

Restrepo-Moreno, S. A., Foster, D. A., Stockli, D. F., & Parra-Sánchez, L. N. (2009). Long-term erosion and exhumation of the "Altiplano Antioqueño", northern Andes (Colombia) from apatite (U–Th)/He thermochronology. *Earth and Planetary Science Letters*, *278*(1–2), 1–12. https://doi.org/10.1016/j.epsl.2008.09.037

Reyes-Harker, A., Ruiz-Valdivieso, C. F., Mora, A., Ramírez-Arias, J. C., Rodriguez, G., de la Parra, F., et al. (2015). Cenozoic paleogeography of the Andean foreland and retroarc hinterland of Colombia. *AAPG Bulletin*, *99*(08), 1407–1453. https://doi.org/10.1306/06181411110

Rooney, T. O., Morell, K. D., Hidalgo, P., & Fraceschi, P. (2015). Magmatic consequences of the transition from orthogonal to oblique subduction in Panama. *Geochemistry, Geophysics, Geosystems*, *16*(12), 4178–4208. https://doi.org/10.1002/2015gc006150

Rosero, A., Carrero, M., Ceballos, C., & Mora, A. (2022). *Seismic and structural analysis of the San Francisco oil field (Colombia). Structural controls on a complex hydrocarbon charge history, Andean Structural Styles* (pp. 195–206). Elsevier.

Sallarès, V., Charvis, P., Flueh, E. R., & Bialas, J. (2003). Seismic structure of Cocos and Malpelo Volcanic Ridges and implications for hot spot-ridge interaction. *Journal of Geophysical Research*, *108*(B12), 2564. https://doi.org/10.1029/2003jb002431

Sánchez, J., Horton, B. K., Tesón, E., Mora, A., Ketcham, R. A., & Stockli, D. F. (2012). Kinematic evolution of Andean fold-thrust structures along the boundary between the eastern cordillera and middle Magdalena Valley basin, Colombia. *Tectonics*, *31*(3), TC3008. https://doi.org/10.1029/2011tc003089

Saylor, J. E., Horton, B. K., Stockli, D. F., Mora, A., & Corredor, J. (2012). Structural and thermochronological evidence for Paleogene basement-involved shortening in the axial Eastern Cordillera, Colombia. *Journal of South American Earth Sciences*, *39*, 202–215. https://doi.org/10.1016/j.jsames.2012.04.009

Schütte, P., Chiaradia, M., & Beate, B. (2010). Geodynamic controls on Tertiary arc magmatism in Ecuador: Constraints from U–Pb zircon geochronology of Oligocene–Miocene intrusions and regional age distribution trends. *Tectonophysics*, *489*(1–4), 159–176. https://doi.org/10.1016/j.tecto.2010.04.015

Seton, M., Müller, R. D., Zahirovic, S., Gaina, C., Torsvik, T., Shephard, G., et al. (2012). Global continental and ocean basin reconstructions since 200 Ma. *Earth-Science Reviews*, *113*(3–4), 212–270. https://doi.org/10.1016/j.earscirev.2012.03.002

Siebert, L., Simkin, T., & Kimberly, P. (2011). *Volcanoes of the World*. Univ of California Press.

Silva, A., Mora, A., Caballero, V., Rodriguez, G., Ruiz, C., Moreno, N., et al. (2013). *Basin compartmentalization and drainage evolution during rift inversion: Evidence from the Eastern Cordillera of Colombia* (Vol. 377, p. 369). Geological Society, London, Special Publications.

Sinton, C. W., Duncan, R. A., Storey, M., Lewis, J., & Estrada, J. J. (1998). An oceanic flood basalt province within the Caribbean plate. *Earth and Planetary Science Letters*, *155*(3–4), 221–235. https://doi.org/10.1016/s0012-821x(97)00214-8

Siravo, G., Faccenna, C., Gérault, M., Becker, T. W., Fellin, M. G., Herman, F., & Molin, P. (2019). Slab flattening and the rise of the eastern cordillera, Colombia. *Earth and Planetary Science Letters*, *512*, 100–110. https://doi.org/10.1016/j.epsl.2019.02.002

Somoza, R., & Ghidella, M. E. (2012). Late Cretaceous to recent plate motions in western South America revisited. *Earth and Planetary Science Letters*, *331–332*, 152–163. https://doi.org/10.1016/j.epsl.2012.03.003

Sun, M., Bezada, M. J., Cornthwaite, J., Prieto, G. A., Niu, F., & Levander, A. (2022). Overlapping slabs: Untangling subduction in NW South America through finite-frequency teleseismic tomography. *Earth and Planetary Science Letters*, *577*, 117253. https://doi.org/10.1016/j.epsl.2021.117253

Syracuse, E. M., Maceira, M., Prieto, G. A., Zhang, H., & Ammon, C. J. (2016). Multiple plates subducting beneath Colombia, as illuminated by seismicity and velocity from the joint inversion of seismic and gravity data. *Earth and Planetary Science Letters*, *444*, 139–149. https://doi.org/10.1016/j.epsl.2016.03.050

Taboada, A., Rivera, L. A., Fuenzalida, A., Cisternas, A., Philip, H., Bijwaard, H., et al. (2000). Geodynamics of the northern Andes: Subductions and intracontinental deformation (Colombia). *Tectonics*, *19*(5), 787–813. https://doi.org/10.1029/2000tc900004

Tatsumi, Y., & Eggins, S. (1995). Subduction zone magmatism. In *Frontiers in Earth Science*. Blackwell.

Tesón, E., Mora, A., Silva, A., Namson, J., Teixell, A., Castellanos, J., et al. (2013). Relationship of Mesozoic graben development, stress, shortening magnitude, and structural style in the Eastern Cordillera of the Colombian Andes. *Geological Society, London, Special Publications*, *377*(1), 257–283. https://doi.org/10.1144/sp377.10

Toda, S., Stein, R. S., Kirby, S. H., & Bozkurt, S. B. (2008). A slab fragment wedged under Tokyo and its tectonic and seismic implications. *Nature Geoscience*, *1*(11), 771–776. https://doi.org/10.1038/ngeo318

Trenkamp, R., Kellogg, J. N., Freymueller, J. T., & Mora, H. P. (2002). Wide plate margin deformation, southern Central America and Northwestern South America, CASA GPS observations. *Journal of South American Earth Sciences*, *15*(2), 157–171. https://doi.org/10.1016/s0895-9811(02)00018-4

Trumbull, R. B., Riller, U., Oncken, O., Scheuber, E., Munier, K., & Hongn, F. (2006). *The time-space distribution of Cenozoic volcanism in the South-central Andes: A new data compilation and some tectonic implications, the Andes* (pp. 29–43). Springer.

Vargas, C. A. (2019). Subduction geometries in Northwestern South America. In *The geology of Colombia* (Vol. 4, p. 397–422). https://doi.org/10.32685/pub.esp.38.2019.11

Vargas, C. A., & Mann, P. (2013). Tearing and breaking off of subducted slabs as the result of collision of the Panama Arc-indenter with Northwestern South America. *Bulletin of the Seismological Society of America*, *103*(3), 2025–2046. https://doi.org/10.1785/0120120328

Veloza, G., Styron, R., & Taylor, M. (2012). *Open-source archive of active faults for northwest South America* (Vol. 22). GSA TODAY.

Villagomez, D., & Spikings, R. (2013). Unraveling the complex interaction between the southern Caribbean, Northwest South America and the Pacific plates during the Cenozoic (p. T22A-08).

Villagómez, D., Spikings, R., Magna, T., Kammer, A., Winkler, W., & Beltrán, A. (2011). Geochronology, geochemistry and tectonic evolution of the Western and Central cordilleras of Colombia. *Lithos*, *125*(3–4), 875–896. https://doi.org/10.1016/j.lithos.2011.05.003

Von Huene, R., & Scholl, D. W. (1991). Observations at convergent margins concerning sediment subduction, subduction erosion, and the growth of continental crust. *Reviews of Geophysics*, *29*(3), 279–316. https://doi.org/10.1029/91rg00969

Wagner, L. S., Jaramillo, J. S., Ramírez-Hoyos, L. F., Monsalve, G., Cardona, A., & Becker, T. W. (2017). Transient slab flattening beneath Colombia. *Geophysical Research Letters*, *44*(13), 6616–6623. https://doi.org/10.1002/2017gl073981

Weber, M., Duque, J. F., Hoyos, S., Cárdenas-Rozo, A. L., Gómez, J., & Wilson, R. (2020). The Combia volcanic province: Miocene post–collisional magmatism in the northern Andes. In *The geology of Colombia* (Vol. 3, pp. 355–394).

Wegner, W., Wörner, G., Harmon, R. S., & Jicha, B. R. (2011). Magmatic history and evolution of the central American land Bridge in Panama since Cretaceous times. *GSA Bulletin*, *123*(3–4), 703–724. https://doi.org/10.1130/b30109.1

Werner, R., Hoernle, K., Barckhausen, U., & Hauff, F. (2003). Geodynamic evolution of the Galápagos hot spot system (Central East Pacific) over the past 20 m.y.: Constraints from morphology, geochemistry, and magnetic anomalies. *Geochemistry, Geophysics, Geosystems*, *4*(12), 1108. https://doi.org/10.1029/2003gc000576

Wilson, D. S., & Hey, R. N. (1995). History of rift propagation and magnetization intensity for the Cocos-Nazca spreading Center. *Journal of Geophysical Research*, *100*(B6), 10041–10056. https://doi.org/10.1029/95jb00762

Yarce, J., Monsalve, G., Becker, T. W., Cardona, A., Poveda, E., Alvira, D., & Ordoñez-Carmona, O. (2014). Seismological observations in Northwestern South America: Evidence for two subduction segments, contrasting crustal thicknesses and upper mantle flow. *Tectonophysics*, *637*, 57–67. https://doi.org/10.1016/j.tecto.2014.09.006

Zapata, S., Zapata-Henao, M., Cardona, A., Jaramillo, C., Silvestro, D., & Oboh-Ikuenobe, F. (2021). Long-term topographic growth and decay constrained by 3D thermo-kinematic modeling: Tectonic evolution of the Antioquia Altiplano, Northern Andes. *Global and Planetary Change*, *203*, 103553. https://doi.org/10.1016/j.gloplacha.2021.103553

Zarifi, Z., Havskov, J., & Hanyga, A. (2007). An insight into the Bucaramanga nest. *Tectonophysics*, *443*(1–2), 93–105. https://doi.org/10.1016/j.tecto.2007.06.004

Zhang, T., Gordon, R. G., Mishra, J. K., & Wang, C. (2017). The Malpelo Plate Hypothesis and implications for nonclosure of the Cocos-Nazca-Pacific plate motion circuit. *Geophysical Research Letters*, *44*(16), 8213–8218. https://doi.org/10.1002/2017gl073704

Zheng, Y., Chen, Y., Dai, L., & Zhao, Z. (2015). Developing plate tectonics theory from oceanic subduction zones to collisional orogens. *Science China Earth Sciences*, *58*(7), 1045–1069. https://doi.org/10.1007/s11430-015-5097-3

References From the Supporting Information

Anderson, V. J., Horton, B. K., Saylor, J. E., Mora, A., Tesón, E., Breecker, D. O., & Ketcham, R. A. (2016). Andean topographic growth and basement uplift in southern Colombia: Implications for the evolution of the Magdalena, Orinoco, and Amazon river systems. *Geosphere*, *12*(4), 1235–1256. https://doi.org/10.1130/ges01294.1

Ayala-Calvo, R., Bayona, G., Cardona, A., Ojeda, C., Montenegro, O. C., Montes, C., et al. (2012). The paleogene synorogenic succession in the northwestern Maracaibo block: Tracking intraplate uplifts and changes in sediment delivery systems. *Journal of South American Earth Sciences*, *39*, 93–111. https://doi.org/10.1016/j.jsames.2012.04.005

Bayona, G., Cortés, M., Jaramillo, C., Ojeda, G., Aristizabal, J. J., & Reyes-Harker, A. (2008). An integrated analysis of an orogen–sedimentary basin pair: Latest Cretaceous–Cenozoic evolution of the linked Eastern Cordillera orogen and the Llanos foreland basin of Colombia. *GSA Bulletin*, *120*(9–10), 1171–1197. https://doi.org/10.1130/b26187.1

Bustamante, C., Cardona, A., Archanjo, C. J., Bayona, G., Lara, M., & Valencia, V. (2017). Geochemistry and isotopic signatures of Paleogene plutonic and detrital rocks of the Northern Andes of Colombia: A record of post-collisional arc magmatism. *Lithos*, *277*, 199–209. https://doi.org/10.1016/j.lithos.2016.11.025

Egbue, O., & Kellogg, J. (2010). Pleistocene to present north Andean "escape". *Tectonophysics*, *489*(1–4), 248–257. https://doi.org/10.1016/j.tecto.2010.04.021

Egbue, O., Kellogg, J., Aguirre, H., & Torres, C. (2014). Evolution of the stress and strain fields in the Eastern Cordillera, Colombia. *Journal of Structural Geology*, *58*, 8–21. https://doi.org/10.1016/j.jsg.2013.10.004

Gómez, E., Jordan, T. E., Allmendinger, R. W., & Cardozo, N. (2005). Development of the Colombian foreland-basin system as a consequence of diachronous exhumation of the northern Andes. *Geological Society of America Bulletin*, *117*(9–10), 1272–1292. https://doi.org/10.1130/b25456.1

Jiménez, G., Rico, J., Bayona, G., Montes, C., Rosero, A., & Sierra, D. (2012). Analysis of curved folds and fault/fold terminations in the southern Upper Magdalena Valley of Colombia. *Journal of South American Earth Sciences*, *39*, 184–201. https://doi.org/10.1016/j.jsames.2012.04.006

Kellogg, J., Ojeda, G., Duque, H., & Ceron, J. (2005). Crustal structure of the eastern Cordillera, Colombia. In *Paper presented at 6th International Symposium on Andean Geodynamics* (pp. 12–14).

Kellogg, J. N., Vega, V., Stallings, T. C., & Aiken, C. L. (1995). Tectonic development of Panama, Costa Rica, and the Colombian Andes: Constraints from global positioning system geodetic studies and gravity. *Special Papers - Geological Society of America*, *295*, 75–90. https://doi.org/10.1130/SPE295-p75

Lara, M., Salazar-Franco, A. M., & Silva-Tamayo, J. C. (2018). Provenance of the Cenozoic siliciclastic intramontane Amagá Formation: Implications for the early Miocene collision between Central and South America. *Sedimentary Geology*, *373*, 147–162. https://doi.org/10.1016/j.sedgeo.2018.06.003

León, S., Monsalve, G., & Bustamante, C. (2021). How much did the Colombian Andes rise by the collision of the Caribbean oceanic plateau? *Geophysical Research Letters*, *48*(7), e2021GL093362. https://doi.org/10.1029/2021gl093362

Montes, C., Guzmán, G., Bayona, G., Cardona, A., Valencia, V., & Jaramillo, C. (2010). Clockwise rotation of the Santa Marta massif and simultaneous Paleogene to Neogene deformation of the Plato-San Jorge and Cesar-Ranchería basins. *Journal of South American Earth Sciences*, *29*(4), 832–848. https://doi.org/10.1016/j.jsames.2009.07.010

Moreno, C. J., Horton, B. K., Caballero, V., Mora, A., Parra, M., & Sierra, J. (2011). Depositional and provenance record of the Paleogene transition from foreland to hinterland basin evolution during Andean orogenesis, northern Middle Magdalena Valley Basin, Colombia. *Journal of South American Earth Sciences*, *32* (3), 246–263. https://doi.org/10.1016/j.jsames.2011.03.018

Nie, J., Horton, B. K., Saylor, J. E., Mora, A., Mange, M., Garzione, C. N., et al. (2012). Integrated provenance analysis of a convergent retroarc foreland system: U–Pb ages, heavy minerals, Nd isotopes, and sandstone compositions of the Middle Magdalena Valley basin, northern Andes, Colombia. *Earth-Science Reviews*, *110*(1–4), 111–126. https://doi.org/10.1016/j.earscirev.2011.11.002

Ortiz, J., Mora, A., Martínez, J., Valencia, A., Gelvez, J., Sanchez, O. & Quintero, I. (2022). Seismic expression of transpressional thick-skinned deformation in the southern foothills of Colombia. In *Andean Structural Styles* (pp. 165–179). Elsevier.

Parnaud, F., Gou, Y., Pacual, J. C., Capello, M. A., Truskowski, I., & Passalacqua, H. (1995). Stratigraphic synthesis of western Venezuela.

Parra, M., Mora, A., Lopez, C., Ernesto Rojas, L., & Horton, B. K. (2012). Detecting earliest shortening and deformation advance in thrust belt hinterlands: Example from the Colombian Andes. *Geology*, *40*(2), 175–178. https://doi.org/10.1130/g32519.1

Piraquive, A., Pinzón, E., Kammer, A., Bernet, M., & von Quadt, A. (2018). Early Neogene unroofing of the Sierra Nevada de Santa Marta, as determined from detrital geothermochronology and the petrology of clastic basin sediments. *GSA Bulletin*, *130*(3–4), 355–380. https://doi.org/10.1130/b31676.1

Ramon, J. C., & Rosero, A. (2006). Multiphase structural evolution of the western margin of the Girardot subbasin, Upper Magdalena Valley, Colombia. *Journal of South American Earth Sciences*, *21*(4), 493–509. https://doi.org/10.1016/j.jsames.2006.07.012

Reyes-Santos, J. P., Mantilla-Monsalve, M., & Gonzalez, J. S. (2000). Regiones Tectono-Sedimentarias del Valle Inferior del Magdalena, Colombia [PAPER IN Spanish] Tectono-Sedimentary Regions of the Lower Magdalena Valley, Colombia.

Saeid, E., Bakioglu, K. B., Kellogg, J., Leier, A., Martinez, J. A., & Guerrero, E. (2017). Garzón Massif basement tectonics: Structural control on evolution of petroleum systems in upper Magdalena and Putumayo basins, Colombia. *Marine and Petroleum Geology*, *88*, 381–401. https://doi.org/10.1016/j.marpetgeo.2017.08.035

Silva-Tamayo, J. C., Sierra, G. M., & Correa, L. G. (2008). Tectonic and climate driven fluctuations in the stratigraphic base level of a Cenozoic continental coal basin, northwestern Andes. *Journal of South American Earth Sciences*, *26*(4), 369–382. https://doi.org/10.1016/j.jsames.2008.02.001

Spikings, R. A., Crowhurst, P. V., Winkler, W., & Villagomez, D. (2010). Syn- and post-accretionary cooling history of the Ecuadorian Andes constrained by their in-situ and detrital thermochronometric record. *Journal of South American Earth Sciences*, *30*(3–4), 121–133. https://doi.org/10.1016/j.jsames.2010.04.002

Spikings, R. A., Winkler, W., Seward, D., & Handler, R. (2001). Along-strike variations in the thermal and tectonic response of the continental Ecuadorian Andes to the collision with heterogeneous oceanic crust. *Earth and Planetary Science Letters*, *186*(1), 57–73. https://doi.org/10.1016/s0012-821x(01)00225-4

van der Lelij, R., Spikings, R., & Mora, A. (2016). Thermochronology and tectonics of the Mérida Andes and the Santander massif, NW South America. *Lithos*, *248*, 220–239. https://doi.org/10.1016/j.lithos.2016.01.006

Villamizar Escalante, N. (2017). Historia de exhumación del bloque este de la falla de Bucaramanga usando termocronología de baja temperatura. Geología.

Wolaver, B. D., Coogan, J. C., Horton, B. K., Bermudez, L. S., Sun, A. Y., Wawrzyniec, T. F., et al. (2015). Structural and hydrogeologic evolution of the Putumayo basin and adjacent fold-thrust belt, Colombia. *AAPG Bulletin*, *99*(10), 1893–1927. https://doi.org/10.1306/05121514186